Metal oxide functionalized nanoporous gold catalysts for hydrogen production

Dissertation

Zur Erlangung des Doktorgrades der Naturwissenschaften

– Dr. rer. nat. –

Vorgelegt dem Promotionsausschuss

des Fachbereichs 2 (Chemie/Biologie)

der Universität Bremen

von

Junjie Shi

Bremen, im Juni 2017

Erstgutachter: Prof. Dr. Marcus Bäumer (Universität Bremen)

Zweitgutachter: Prof. Dr. Thomas Risse (Freie Universität Berlin)

Selbstständigkeitserklärung

Hiermit erkläre ich, dass ich die vorliegende Arbeit selbständig angefertigt und keine außer den angegebenen Hilfsmitteln verwendet habe. Diese Arbeit wurde nicht vorher an anderer Stelle eingereicht.

Bremen, den

_____

(Junjie Shi)

I am indebted to the following people and institutions for supporting me during my PhD project:

Prof. Dr. Marcus Bäumer: Thank you for offering me this valuable opportunity to study in Germany, it opens up a new window for me in my life. Thank you for providing me such a good platform and the opportunities to communicate with so many intelligent colleagues. Thank you for the helpful discussions and assistance in the process of preparing all my papers and dissertation. Your open mind, extensive knowledge and approachable attitude to the students impressed me deeply.

Prof. Dr. Thomas Risse: Thank you very much for being my second reviewer. Thank you for your valuable time and effort to review my PhD work.

Dr. Arne Wittstock: Thank you so much for guiding and supporting me during my study in IAPC. As my direct supervisor, I really learn a lot from you. Thank you for patiently teaching me how to organize a presentation, how to write the research papers and how to do research... Your rigorous attitude to science and encouragement to me will always remain in my mind.

Prof. Dr. Thorsten M. Gesing and Dr. M. Mangir Murshed: Thank you for your help in the Raman characterization and the scientific discussion on data.

Prof. Dr. Andreas Rosenauer and Christoph Mahr: Thank you for your help in the TEM characterization and the scientific discussion on data.

Priv. Doz. Dr. Volkmar Zielasek: Thank you for your professional support in the TEM measurement and analysis. Thank you for helping me correct the powerpoint for ACS meeting and doing the proof reading for my thesis.

Martin Novak: Thank you for the technical support in building my experimental equiment **and Connie Rybarsch:** Thank you for helping me order all the chemicals and it is always interesting to chat with you. **Dr. Günter Schnurpfeil:** Thank you for patiently helping me preparing the TEM samples. Especially I would like to thank my "roommate" **Anastasia Lackmann:** Thank you for your company. We have so many nice conversations and thank you for doing the surface area measurement for my sample.

All the IAPC group members: **Dr. Lyudmila Moskaleva, Simona Keil, Imke Schrader, Dr. Sebastian Kunz, Dr. Andreas Schaefer, Vera Suling, David Steinebrunner, Yong Li, Miriam Schubert, Stefan Wild, Sarah Neumann, Brigitte Neimeier** and the former **(Willian Menezes, Björn Neumann, Lena Altmann, Melanie Minnermann, Andre Wichmann, Ingo Bardenhagen, Jin-Hao Jhang, Theodor Weiss, Darius Arndt, Sarah**

Röhe) : Thank you for providing me a relaxed and pleasant working environment. It was my pleasure working with you.

I would like to thank my friends Pengfei Qi, Shuwen Sun, Li Wang, Yan Wang, Debo Wu and G. D. Maier, thank you for your support and company.

Last but not the least, I would like to thank my parents for all their love and encouragement.

I gratefully acknowledge the China Scholarship Committee (CSC) for providing the major financial support for my stay in Germany. I would also thank Bremen University for providing me the international meeting scholarship and STIBET graduation scholarship. In the end my work I was also supported by German Research Foundation (DFG) with project: Nanoporous Gold as new catalyst material (SP 2) from Dr. Arne Wittstock's part.

This thesis is based on the following papers, which will be referred to in the text by their roman numerals:

(Ⅰ) **Nanoporous Gold-Supported Ceria for the Water–Gas Shift Reaction:UHV Inspired Design for Applied Catalysis**
Junjie Shi, Andreas Schaefer, Andre Wichmann, M. Mangir Murshed, Thorsten M. Gesing, Arne Wittstock, and Marcus Bäumer
J. Phys. Chem. C, 2014, Volume: 118, Issue:50, Pages: 29270–29277
http://pubs.acs.org/doi/abs/10.1021/jp505433a

(Ⅱ) **A versatile sol-gel coating for mixed oxides on nanoporous gold and their application in the water gas shift reaction**
Junjie Shi, Christoph Mahr, M. Mangir Murshed, Volkmar Zielasek, Andreas Rosenauer, Thorsten M. Gesing, Marcus Bäumer and Arne Wittstock
Catal. Sci. Technol., 2016, Issue: 6, Pages: 5311-5319
http://pubs.rsc.org/en/content/articlelanding/2016/cy/c5cy02205c#!divAbstract

(Ⅲ) **Steam Reforming of Methanol over Nanoporous Gold/Oxide Catalysts: A Combined In-situ FTIR and Flow Reactor Study**
Junjie Shi, Christoph Mahr, M. Mangir Murshed, Thorsten M. Gesing, Andreas Rosenauer, Marcus Bäumer, Arne Wittstock
Phys. Chem. Chem. Phys., 2017, Issue: 19, Pages: 8880-8888
http://pubs.rsc.org/en/content/articlepdf/2017/cp/c6cp08849j

In addition to my own PhD project, I was also involved in additional research activities:

(Ⅳ) **In Situ Ptychography of Heterogeneous Catalysts using Hard X-Rays: High Resolution Imaging at Ambient Pressure and Elevated Temperature**
Sina Baiera, Christian D. Damsgaard, Maria Scholz, Federico Benzi, Amélie Rochet, Robert Hoppe, Torsten Scherer, Junjie Shi, Arne Wittstock, Britta Weinhausen, Jakob B. Wagner, Christian G. Schroer and Jan-Dierk Grunwaldt
Microscopy and Microanalysis, 2016, Volume: 22, Issue: 01, Pages: 178-188
http://journals.cambridge.org/action/displayAbstract?fromPage=online&aid=10197740&fileId=S1431927615015573

(Ⅴ) **Influence of gas atmosphere and ceria on the stability of nanoporous gold studied by environmental electron microscopy and in situ ptychograph**
Sina Baier, Arne Wittstock, Christian D. Damsgaard, Ana Diaz, Juliane Reinhardt, Federico Benzi, Junjie Shi, Torsten Scherer, Di Wang, Christian Kübel, Christian G. Schroer and Jan-Dierk Grunwaldt.
RSC Advances, 2016, Issue: 6, Pages: 83031-83043
http://pubs.rsc.org/en/content/articlepdf/2016/RA/C6RA12853J

Statement regarding my contribution to the published work:

All stated publications are unexceptionally based on the collaboration of several researchers.

Nevertheless, for *publication* ***(I)*** I was responsible for writing the manuscript, designing the experiments, the preparation of samples, and for the complete catalytic characterization of samples. Andreas Schaefer carried out the XPS characterizations. M. Mangir Murshed carried out the Raman characterizations. Arne Wittstock and Marcus Bäumer were involved in discussing and analyzing the results. All authors commented on the manuscript.

Regarding *publication* ***(II)*** I was responsible for writing the manuscript, designing the experiments, the preparation of samples, and for the complete catalytic characterization of samples. Christoph Mahr and Volkmar Zielasek carried out the TEM characterizations. M. Mangir Murshed carried out the Raman characterizations. Arne Wittstock and Marcus Bäumer were involved in discussing and analyzing the results. All authors commented on the manuscript.

For *publication* ***(III)*** I was responsible for writing the manuscript, designing the experiments, the preparation of samples, and for the complete catalytic characterization of samples. Christoph Mahr carried out the TEM characterizations. M. Mangir Murshed carried out the Raman characterizations. Arne Wittstock and Marcus Bäumer were involved in discussing and analyzing the results. All authors commented on the manuscript.

For *publication* ***(IV)*** I was responsible for preparing the npAu and oxides functionalized npAu samples and contributed to the preparation of the manuscript.

For *publication* ***(V)*** I was responsible for preparing the npAu and oxide-functionalized npAu samples and contributed to the preparation of the manuscript.

Zusammenfassung

Nanoporöses Gold (npAu) hat viele Anwendungsmöglichkeiten – insbesondere in der heterogenen Katalyse. Als Katalysator weist npAu schon hohe Reaktivität bei niedrigen Temperaturen (ab 20°C) auf. Allerdings wird die praktische Anwendung durch Vergröberung seiner 3D-Struktur bei hohen Temperaturen (> 100°C) stark eingeschränkt, da dies zum Verlust der katalytisch aktiven Oberfläche führt. Zur Lösung dieses Problems wurde in dieser Arbeit ein Nasseimprägnierungsverfahren und ein Sol-Gel-Verfahren zur Beschichtung von dispergierten Oxid-Nanopartikeln auf npAu entwickelt. Neben der drastischen Verbesserung der thermischen Stabilität und der mechanischen Eigenschaften von npAu eröffnete die Funktionalisierung eine Reihe neuer Anwendungen, wie z.B. Wasser-Gas-Shift-Reaktion (WGSR) und die Dampfreformierung von Methanol (SRM). Im Mittelpunkt dieser Arbeit steht die Untersuchung der Wirkung von Oxidzugabe auf npAu im Hinblick auf die chemische Reaktivität des Systems, um die Ursprünge der katalytischen Aktivität von oxid-funktionalisierten npAu zu verstehen.

Ein inverser Ceroxid/npAu-Katalysator (CeO_x/npAu) wurde zuerst durch eine Naßimprägnierung mit anschließender thermischer Zersetzung von einer Cernitratverbindung auf einem npAu-Substrat mit Ceroxidbeladungen von etwa 3 bis 10 Atom-% hergestellt. Durch die Anwesenheit von CeO_x konnte die 3D-Struktur von npAu thermisch stabilisiert werden. Danach wurden TiO_2-CeO_2-Mischoxide im npAu-Netzwerk unter Verwendung eines Sol-Gel-Verfahrens untersucht, um die katalytische Aktivität des npAu-basierten inversen Katalysators weiter zu verbessern. Die strukturelle TEM-Charakterisierung der Proben zeigte, dass die Stege der nanoporösen Struktur reichlich mit kleinen Oxidagglomeraten (1 – 2 nm groß) bedeckt sind. Diese Materialien wiesen genauso wie die CeO_x/npAu Katalysatoren eine ausgezeichnete Stabilität und Reproduzierbarkeit bis zu Temperaturen von über 500°C auf.

Raman-Spektroskopie wurde verwendet, um Interaktionen von verschiedenen

Gasen (O_2, H_2O, CO) mit dem oxid-funktionalisierten npAu zu verstehen. Die Charakterisierung der Kristallinität und des Verhaltens von Sauerstoffleerstellen in den Oxiddeponaten im npAu unter verschiedenen Gasbedingungen (O_2, H_2O, CO) zeigte, dass eine dynamische Korrelation zwischen der Kristallstruktur (Sauerstoffspeicherung) der Metalloxide und den oxidierenden und reduzierenden Bedingungen besteht, was auch bedeutet, dass die Oxidzugaben die chemische Reaktivität des Systems wirksam verbessern könnten.

Untersuchungen zur Wassergas-Shift-Reaktion an CeO_x/npAu zeigte die Bildung von CO_2 bei Temperaturen von nur 135°C. Der Aktivitätsverlust betrug nur etwa 10% nach ca. 15 h katalytischer Anwendung bei 535°C. Die photoelektronenspektroskopische Charakterisierung des Materials zeigte, dass ein Defekt von (Ce^{3+}) eine Schlüsselrolle bei der Dissoziation von H_2O spielt. Durch den Vergleich der katalytischen Aktivitäten verschiedener Katalysatoren wurde festgestellt, dass die $Ce_1Ti_2O_x$/npAu-Probe die höchste Aktivität zeigte, die fast doppelt so hoch war wie die Aktivität aller anderen Proben bei 300 °C. Dies kann mit der hohen Dissoziationsfähigkeit des Katalysators für Wasser erklärt werden.

Zusätzlich zu WGS wurde ein weiterer wichtiger Wasserstoffproduktionsprozess untersucht: die Dampfreformierung von Methanol (SRM). Die Durchflussreaktor-Studie zeigte, dass sowohl CeO_x/npAu als auch $Ce_1Ti_2O_x$/npAu eine hohe Aktivität und Selektivität für die Reformierungsreaktion aufweisen.

Um die katalytischen Eigenschaften von oxid-funktionalisiertem npAu hinsichtlich der WGS und SRM mechanistisch zu verstehen, wurden Photoelektronenspektroskopie und diffuse Reflexions-Infrarot-Spektroskopie (DRIFT) verwendet. Die Untersuchungen zeigen, dass die Aktivierung von Wasser und die Bildung von OH_{ads} der Schlüssel zur Aktivität / Selektivität der Katalysatoren sind.

Abstract

Nanoporous gold (npAu) has shown potential for applications in many fields, in particular for heterogeneous catalysis. Much progress has been made in utilizing the high reactivity of npAu catalysts for selective oxidation reactions at low temperatures. However, its tendency to coarsen at high temperatures severely limits the practical applications of npAu, as it results in the loss of catalytically active surface. To solve this problem, we explored a wetness impregenation method and a sol–gel method in order to deposit dispersed oxide nanoparticles on npAu. In addition to drastically improving the thermal stability and mechanical properties of npAu, the functionalization opens up a range of new and beforehand unseen applications, for example, for hydrogen production reactions, such as the water gas shift reaction (WGSR) and steam reforming of methanol (SRM). The focus of the present work was to investigate the effect of adding oxide deposites on npAu and to understand the origins of the catalytic activity of these systems.

An inverse ceria/npAu catalysts was first prepared by wet impregnation and thermal decomposition of a cerium nitrate precursor on a npAu substrate. The ceria loadings were about 3 to 10 atom %. The presence of ceria oxide on the nanosized gold ligaments play a key role in helping to increase the thermal stability of the material. Subsequently, a series of TiO_2-CeO_2 mixed oxides was synthesized inside the npAu network using a sol–gel method in order to further improve the catalytic activity of the npAu-based inverse catalyst. The structural characterization of the samples with TEM indicated that the gold ligaments were abundantly covered by small oxide agglomerates with sizes of about 1–2 nm. These materials exhibited similar properties as compared to ceria functionalized npAu, i.e. showed excellent stability and reproducibility up to temperatures of over 500°C.

Raman spectroscopy has been used to study interactions of different gases (O_2, H_2O, CO) with the oxide functionalized npAu samples. The characterization of the

crystallinity and the behavior of oxygen vacancies in the npAu supported metal oxides under different gases conditions (O_2, H_2O, CO) indicated that there is a dynamic correlation between the crystallization (oxygen storage) of the metal-oxides and the oxidizing and reducing conditions, which also implies that the addition of oxide deposits can effectively improve the chemical reactivity of the system.

Water-gas shift (WGS) reaction tests on CeO_x/npAu showed formation of CO_2 at temperatures as low as 135°C. The loss of activity after about 15 h of catalytic conversion at temperatures up to 535°C was only about 10%. Photoelectron spectroscopy studies of the material revealed that defect rich ceria (Ce^{3+}) plays a key role in the dissociation of H_2O. By comparing the catalytic activities of different catalysts, it was found that the $Ce_1Ti_2O_x$/npAu sample yields the highest activity which was nearly twice as high as the activity of all other samples at 300°C. This was related to its high dissociation ability for water.

In addition to WGSR, another important hydrogen production process, namely the steam reforming of methanol (SRM), was studied. The reaction of methanol with water yielded hydrogen as a reaction product quantitatively. The flow reactor study showed that both, CeO_x/npAu and $Ce_1Ti_2O_x$/npAu, had a high activity and selectivity for the reforming reaction.

To understand the origins of the catalytic activity of the oxide functionalized npAu, photoelectron spectroscopy and diffuse reflectance infrared spectroscopy (DRIFT) have been used. The investigations revealed that the activation of water and the formation of OH_{ads} are key factors for the different activity/selectivity of the catalysts.

Content

1. Introduction

Novel catalytic materials play a central role for the improvement of processes connected with the conversion of energy, remediation of environmental pollutants, and the synthesis of chemicals and materials.[1-3] One area which witnessed considerable activity in the past decades is hydrogen production. This development was and is driven by the increasing demand for environmentally friendly sources of energy. Accordingly, this trend has led to a worldwide search for better catalysts for hydrogen production.

In heterogeneous catalysis, catalytic metals are largely confined to the elements of groups VIII and IB in the periodic table.[4] There are, however, many large and important differences between the two groups of elements. The excellent catalytic activity of group VIII metals can be attributed to the optimum degree of d-band filling. The elements of group IB, the so called coinage metals (Cu, Ag and Au), have fully occupied d-bands (respectively 3d, 4d and 5d).[4] However, owing to the relatively low ionization potential of Cu and Ag, they can easily lose electrons to yield d-band vacancies; therefore they are potentially able to be catalytically active. In fact, in industry Cu is often used in methanol synthesis and Ag is often used for ethylene oxide synthesis.[5] In contrast, Au has a high ionization potential and therefore a poor affinity towards molecules. Surface science studies and density functional calculations also show that no dissociative adsorption of H_2 and O_2 can happen on the surface of gold below 200°C, which indicates that Au should be catalytically inactive for hydrogenation and oxidation reactions.[5]

For these reasons, gold was regarded as an inactive metal in catalysis for a long time. However, today gold has attracted great interest of both industrial and academic scientists. After 30 years of research some key progress has been made. For example, Hutchings et al. reported that a Au/C catalyst has been commercialized in the acetylene hydrochlorination in industry since 2007.[5]

The recent advent of interest in gold catalysis dates back to the 1980s, when Haruta

and co-workers first reported that nanosized Au clusters prepared by coprecipitation or deposition-precipitation show high catalytic reactivity toward low-temperature CO oxidation.[2, 6] Almost at the same time, nanoporous gold (npAu) as an open-cell metal foam was discovered by scientists when they were studying the corrosion process of Ag-Au alloys through electrochemical techniques.[7] In the next two decades most of the studies were focused on studying dealloying and stress corrosion cracking. Albeit much progress has been achieved in this area, the application of npAu in the field of catalysis has been long over-looked until recently.

In 2006, our group and Ding's group (short time later) independently reported that this "unspported" gold catalyst shows high activity for the low-temperature CO oxidation.[7-10] To a large extent, these findings have refreshed people's understanding of the traditional gold catalyst, because all the previous studies consistently claimed that the catalytic activity of Au catalysts is limited to very small Au particle sizes (<5 nm) and that the interaction with a metal oxide support plays an important role for the observed catalytic activity. Nonetheless, nanoporous gold as a unsupported three-dimensional nanoporous bulk material with much larger feature sizes (10-50 nm), also shows high activity for low-temperature CO oxidation.

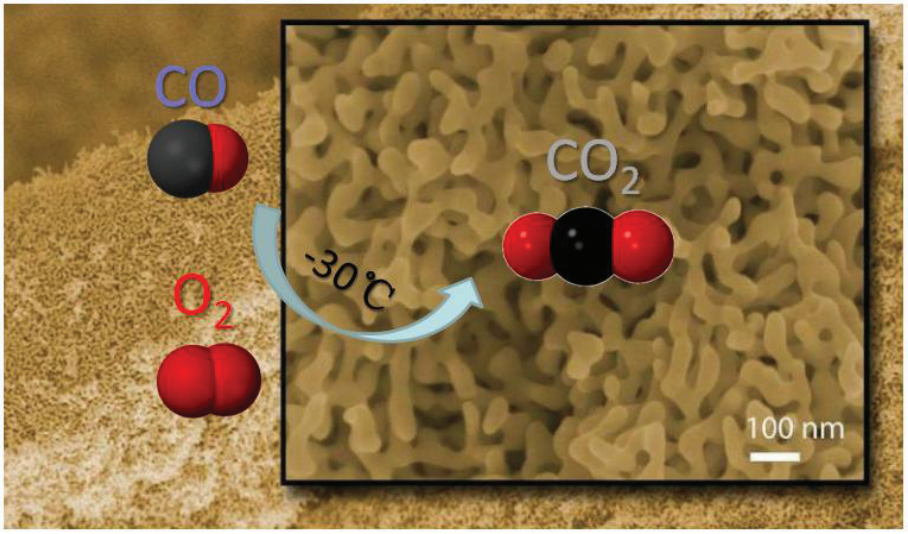

Figure 1. The 3D structure of npAu generated by etching a Au-Ag alloy by concentrated HNO_3. The resulting structure can be characterized as a (open-cell) metal foam with ligaments and pores in the range of tens of nanometers. Inset (middle): The scheme of low temperature CO oxidation. (Modifed from Dr. Arne Wittstock's PhD dissertation)

Nanoporous gold usually is prepared by selective corrosion (dealloying) of a gold alloy containing a less noble constituent, such as silver, copper or aluminum, in analogy to a process by which Raney nickel is made from Ni-Al alloys via leaching out Al.[8, 10-11] After the first report on using npAu as a catalyst for CO oxidation,[9-10] there have been more studies reporting the application of npAu catalysts in other reactions, such as gas-phase and liquid-phase oxidation of alcohols and glucose, electrochemical oxidation of methanol, as well as oxidation of organosilanes with water.[12-17] All these studies have in common that they demonstrate npAu's capability to provide high activity and selectivity, even under relatively mild reaction conditions.

2. Origins of the catalytic activity of nanoporous gold

It is known that bulk metallic gold has a very poor activity for the activation of simple molecules, such as H_2, O_2, CO.[18-19] However, when gold is dispersed in the form of nanometer-sized particles, subnanometer-sized clusters or even single atoms and supported on some high-surface-area oxide or carbon supports, it can exhibit high catalytic activities.[18, 20-21] Numerous experimental and theoretical studies have been conducted to understand the high catalytic activity of supported gold nanoparticles.[22-26] Generally, it is believed that the enhancement of the catalytic activity is related to two effects.

One of the effects is the so called quantum effect/morphological effect—the high abundance of corner and edge atoms on the surface of small particles (< 5 nm).[18] In fact, there are two ways in which corner or edge atoms can influence the reaction, one is electronic and the other one is geometrical by nature.[27] The electronic factor is due to the fact that low-coordinated surface metal atoms have different local electronic structures and thus interact differently with molecules, leading to different adsorption and reaction properties.[27] According to Norskov, the d-band center of transition metals can be used to assess the ability of atoms to form bonds with adsorbates.[27] For example, transition metal atoms with a low coordination number (steps, edges, kinks and corners) usually exhibit higher lying d-states which result in a stronger interaction of these atoms with adsorbates than atoms on close packed terraces. The geometrical factor is due to different surface geometries which provide different surface atom configurations, i.e. adsorption sites for molecules. In general, it is hard to differentiate between these two effects. For example, on the one hand, atomic steps provide atoms with higher-lying d-states. On the other hand, they also provide new surface atom configurations.[27]

The other important effect is the support effect, which also can be divided into two mechanisms. One is called support induced mechanism, by which the support can influence the reactivity of the gold catalyst by charging the gold nanoparticles and/or

inducing strain in the structure.[28] The other effect is called support driven mechanism. Here the enhancing effect results from the fact that O_2 molecules are trapped on the support including mass transport of the reactants to the reaction site.[28] Additionally, the support can stabilize some active species during the reaction process either by polarization effects or by direct bonding.[18, 29]

Nanoporous gold fabricated by electrochemical or free corrosion without any support shows an activity towards many oxidation reactions similar to small, oxide-supported gold nanoparticles.[12, 30-31] In contrast to oxide supported gold catalysts, npAu exhibits a sponge-like open-cell morphology with feature sizes that are much larger (30 to 50 nm) than catalytically active Au nanoparticles.[11] However, similar to nanoparticulate gold, the catalytic activity of npAu also strongly depends on the size of the nanopores or ligaments.[8, 32] Chen et al. reported that a high density of atomic steps and kinks exist on the curved surfaces of npAu, which are comparable to 3–5 nm gold nanoparticles.[30] The DFT results also show that Au tends to be catalytically active for the activation of molecular oxygen when the coordination of atoms is low enough.[7, 18] Therefore, it has been argued that the catalytic activity of npAu is purely an electronic effect; in other words, the activity originates merely from the high density of under-coordinated step and kink sites present on the curved ligament surfaces.[7] (Figure 2)

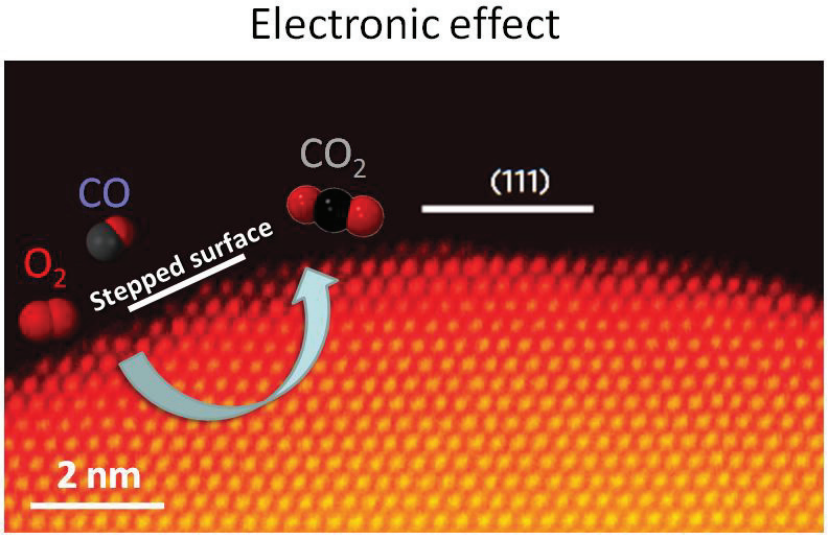

Figure 2. Atomic structure of the surface of np-Au: HAADF-STEM image of convex (111) terraces and neighboring atomic kinks. Reprinted with permission from ref 28, Copyright 2012, Nature Publishing Group.

The low-coordinated Au sites may indeed be important for some reactions, however, another factor that cannot be simply ignored is the residual elements' effect. (Figure 3) It is known that npAu always contains residual less-noble elements that cannot be completely removed by dealloying.[29, 33] Both, experimental observations and theoretical studies, conducted by our working group suggest that catalytic activity of npAu is not only a unique feature of the special surface geometry of the material.[29, 34] It also depends on the distribution of residual Ag and its chemical state on the surface.[29] The studies from Sault et al.[35] on Au(110) and Kim et al.[36] on Au(211) also point to the fact that molecular oxygen cannot be activated on these surfaces (at atmospheric pressure and 300−450 K), although they contain a high density of low coordinated atoms. In addition, studies based on npAu made from $AuCu_3$ alloys (residual Cu content 12−27 at. %) show that residual Cu could also promote the activation of molecular oxygen on npAu.[7] These findings indicate that small concentrations of residual elements/additives on the surface of npAu can play an essential role in influencing the chemical properties of the catalysts. Ideally, one can take advantage of these phenomena when designing highly efficient npAu based catalysts for a broader range of catalytic applications.

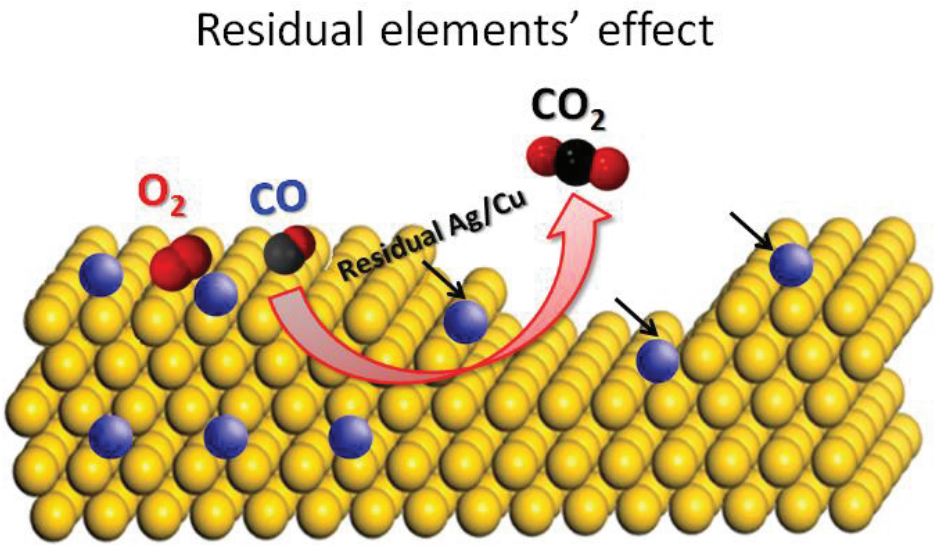

Figure 3. Illustration of the reaction between O_2 and CO diffusion on the stepped npAu surface with residual Ag or Cu atoms helping to dissociate molecular oxygen.

3. Modification of nanoporous gold with metal oxides : A synergistic effect

Metal oxides are one of the most widely employed materials, which can be used either as active catalytic phases or as supports for dispersed catalysts.[37] Their catalytic activity may be ascribed to the presence of acid–base sites and their special redox properties.[37-38] In order to achieve better catalytic performance, i.e. to improve the catalytic activity and selectivity, for example the development of multicomponent composite catalysts is a possible choice. In fact, the combination of noble (Pt, Au, Ru) metals and metal oxides is frequently used in heterogeneous catalysis.[37] Often, the high performance of these catalysts is largely dependent on a possible synergistic catalytic interaction of the metal and the oxide support on the nanoscale.

Synergistic catalytic effects can be defined as a kind of cooperation between different components (active sites) which result in a significantly enhanced catalytic performance as compared to the simple summation of the properties of the individual components.[39] In reality, the cooperations/interactions between different catalyst components are complicated. Based on a thorough study of literature reports and own work on nanocomposite catalysts, Shi proposed that the synergistic catalytic effects can be divided into four different types.[39] A detailed discussion of this field is beyond the scope of the current thesis, but an excellent summary can be found in this review.[39]

Here, we only introduce one type of synergistic catalytic effect, namely the situation that one component is activated by the other. The main feature of this effect is that a second component of a catalyst can initiate or improve the catalytic activity of the main component during the reaction by promoting the formation of a special activated species (e.g., radicals) of the main component. Take the reaction $A + B \rightarrow C$ as a simple example: catalyst α alone has a low kinetic rate or cannot catalyze the reaction, in the following way :

$$A + B \xrightarrow{\alpha} \not\rightarrow C$$

In case of a α/β hybrid catalyst, α can be activated by β to an activated state (α′), according to:

$$\alpha + \beta \longrightarrow \alpha'/\beta$$

Or α and β can be mutually activated to α′ and β′, according to:

$$\alpha + \beta \longrightarrow \alpha'/\beta'$$

Then the α′/β or α′/β′ catalyst formed in these ways can largely accelerate the reaction process:

$$A + B \xrightarrow{\alpha'/\beta} C \quad \text{or} \quad A + B \xrightarrow{\alpha'/\beta'} C$$

This kind of synergistic catalytic effect is prevailing in a lot of catalytic reactions. One typical example are gold catalyzed reactions. The combination of oxides with Au is quite well-known in the field of traditional gold catalysts, with Au nanoparticles supported on metal oxides.[40-42] As mentioned in the last section, in addition to the small dimension and morphology of gold nanoparticles, the catalytic performance is highly dependent on the type of support. Among the numerous supports studied, titania and ceria have been proved to be the most effective supports for Au, catalyzing a variety of reactions. For example, small gold particles dispersed on ceria or titania are excellent catalysts for the water gas shift reaction, selective oxidation of alkenes and alcohols.[39] A schematic illustration of the proposed synergistic catalytic effect, found for Au/CeO_2 or Au/TiO_2 composites is shown in Figure 4. In general, Au promotes the catalytic activity mainly through an electron donation effect. By donating electrons to ceria or titania, the oxide support can be activated by Au by generating Ce(III) from Ce(IV) or TiO_{2-x}, respectively, and at the same time, oxygen vacancies can be created on the surface of the oxides for further oxygen or water activation.

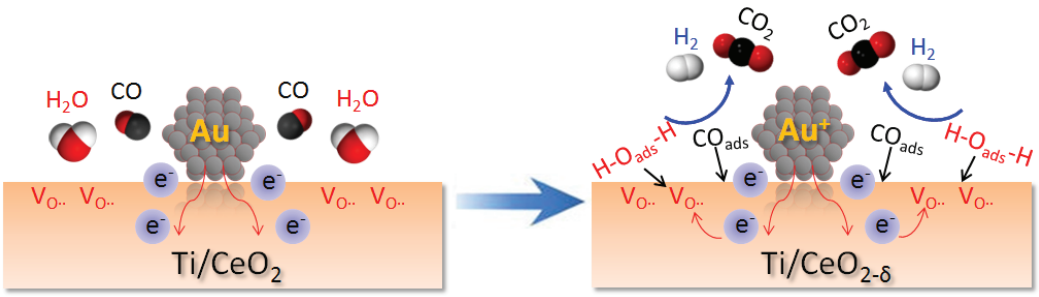

Figure 4. Schematic illustration of the synergistic catalytic effect for Au/CeO_2 or Au/TiO_2 composites: Simply, oxygen vacancies can be generated in CeO_2 or TiO_2 in the presence of reducing agents and especially the promotion of Au via the electron donation effect, and the active O_{ads} species formed at the vacancies can accelerate oxidation/dissociation reactions.

A very large number of studies have been conducted for oxide supported Au nanoparticles systems, however, what happens when inversely nanoparticles of a given metal oxide are deposited on the surface of a Au support? Recently, Rodriguez and co-workers conducted a series of model studies by depositing metal oxides, such as TiO_2 or CeO_2, on Au(111) or Cu(111) surfaces under ultra high vacuum conditions (UHV) and found that such inverse catalysts also show a high catalytic performance for the water-gas shift reaction.[43-45] The inverse system is reported to be even more active than the traditional oxide supported metal particles catalyst.[46] However, this is only limited to an UHV study, the challenge of transferring this inverse design to ambient pressure applications arises from the requirement of a high surface area gold support.

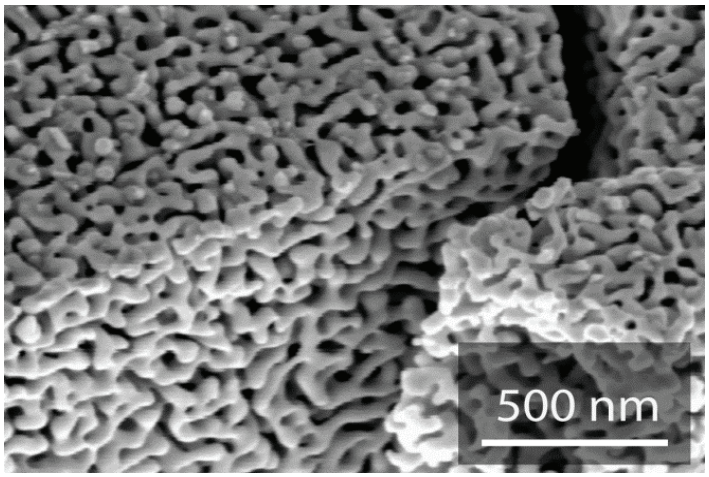

Figure 5. Scanning electron micrograph of a nanoporous gold material, showing the outer surface and a crack along a grain boundary.(Reproduced from publication III, copyright Royal Society of Chemistry, 2017)

The interesting structural features of npAu include a three-dimensional (3D) bicontinuous open pore network structure (Figure 5) on the order of a few tens of nanometers (~40 nm typically), an accordingly high surface-to-volume ratio, specific surface areas between 4−30 m^2/g, i.e. properties which render this material an attractive candidate for novella inverse Au catalyst design. At the same time, the combination of npAu with suitable metal oxides (Figure 6) also offers the opportunity to drastically improve the thermal stability and mechanical properties of npAu.[8, 47-48]

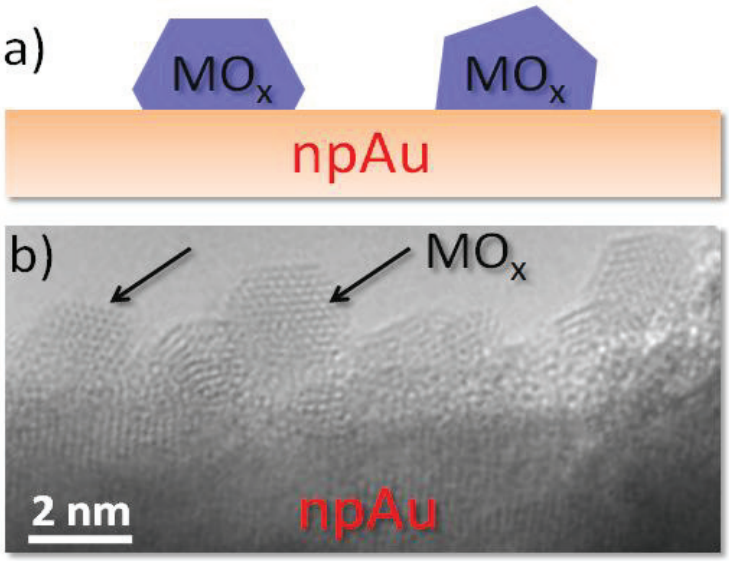

Figure 6. a) Scheme for nanoporous gold modified with metal oxides(MO_x). b) High resolution transmission electron microscopic (HRTEM) images of nanoporous gold coated with titania–ceria mixed oxides ($Ce_1Ti_2O_x$/npAu) after calcination at 450°C in helium for 2h.

3.1 *Fabrication of ceria-functionalized npAu catalysts*

(Relevant papers: I)

Previously, great efforts have been directed toward the synthesis of oxides@npAu structures. For example, Biener and co-workers introduced an atomic layer deposition (ALD) strategy for controlled layer by layer coating on the interior surface of npAu by TiO_2 and Al_2O_3.[47] My co-worker, Andre Wichmann, found that the simple impregnation of npAu with a highly hydrolyzable titaniumisopropoxide (TTIP) solution followed by controlled annealing could also result in a homogeneous distribution of TiO_2 nanoparticles inside the porous structure.[48] In addition, Lang and co-workers have developed a hydrothermal approach to deposite Co_3O_4 inside the npAu nanopore system.[49] However, studies aiming at modifying npAu with metal oxide are still in an initial stage, to date; the reports on the effective preparation of metal oxide deposits on npAu are quite limited, although they exhibit valuable properties for catalyzing certain chemical reactions. Particularly CeO_2, as mentioned above, has shown great potential for the water-gas-shift reaction after depositing it on Au (111) surface. In order to transfer this inverse catalyst design to larger scale ambient pressure conditions, we have prepared a CeO_x functionalized npAu catalyst for ambient WGSR studies. Recent work with respect to the structural characterization of the CeO_x modified npAu system will be briefly introduced in this section.

We use a facile and cost-effective wetness impregnation and pyrolysis method to add ceria onto the surface of npAu. As revealed by scanning electron microscopy and transmission electron microscopy, shown in Figure 7, the ligaments of npAu exhibitting an average ligament size of around 40 nm are uniformly and abundantly covered by ceria deposits. Further investigations with energy dispersive X-ray spectroscopy (EDX) indicated that these deposits consist of cerium oxide with a

content of Ce was between 2-10 atom%. After annealing up to 485°C for over 2 hours most of the gold ligaments and pores kept their diameter of around 40 nm without coarsening. To be mentioned, the partial coarsening in some regions of the sample can be attributed to an inhomogeneous distribution of the precursor inside the porous structure. In general, the finding is in line with prior work of Wichmann et al. on TiO_x functionalized npAu.[11, 48] It is suggested that the stabilization of the Au porous structure at elevated temperatures is related to the presence of the metal oxide deposits on the ligament surface.[11, 48] Because the melting temperature of metal oxides, such as TiO_2 (1843°C) and CeO_2 (2400°C) is much higher than that of gold (1063°C), which also corresponds to a higher Huttig-temperature the metal oxide nanoparticles are considerably more stable against coalescence.[40] Furthermore, the oxide deposits prevent coarsening of the Au ligaments themselves, probably because they hinder diffusion of Au atoms from step edges, a mechanism that is considered to be responsible for the coarsening process.

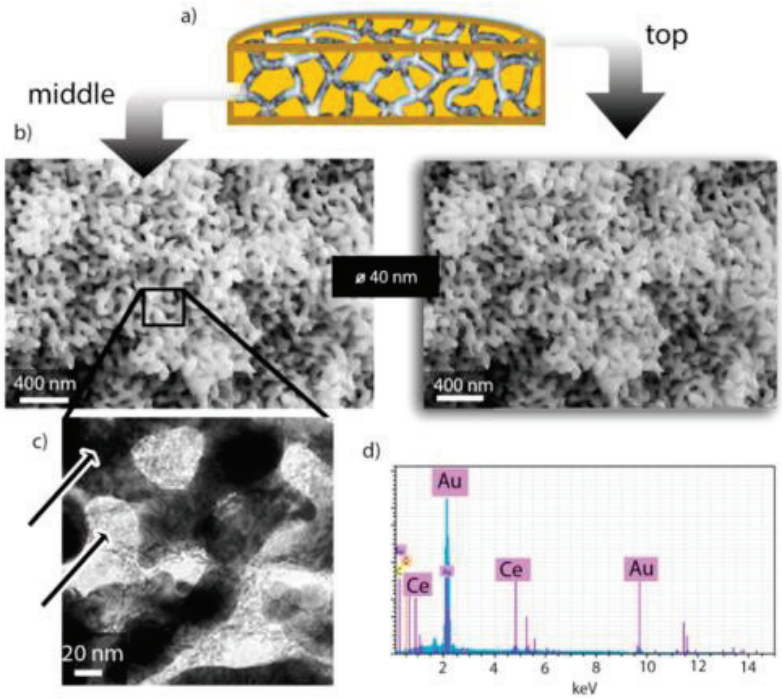

Figure 7. Characterization of cerium oxide-modified nanoporous gold. (a,b) SEM of a freshly cleaved cross section of a CeO_x/npAu disk (~200 µm thick). (c) The cerium oxide deposits become visible at higher magnification (TEM). Arrows indicate the npAu support (upper arrow) and the cerium oxide deposit (lower arrow). (d) EDX confirms that these deposits are cerium oxide on gold (~5 atom% cerium). (Reproduced from publication Ⅰ, copyright American Chemical Society, 2014)

3.2 Fabrication of mixed metal oxide-functionalized npAu catalysts

(Relevant papers: II& III)

Following up on the first studies using npAu as the support for pure CeO_2 oxide deposits, we pursued the question if mixed oxides of CeO_2 and TiO_2 supported on npAu could show even higher WGSR activity. Several studies on TiO_2–CeO_2 mixed oxides have shown improvements regarding redox, textural, and structural properties.[43, 50-57] The incorporation of Ti into the ceria lattice was shown to increase the fraction of partially reduced Ce^{3+} which was shown to be an active site for bonding and dissociation of water.[38, 43, 58] Yet, owing to the active chemical nature of the precursor, the titanium tends to form preferentially pure titania and not mixed oxides, so that it is difficult to control the reaction kinetics for heterogeneous nucleation and growth of mixed oxides on the desired substrate.[59-61]

In view of these issues, we have developed a versatile sol–gel method for coating mixed oxides on nanoporous gold, which allows overcoming all the problems. In the following section, the main aspects of the work will be summarized, emphasizing the fine control over the composition of the mixed oxides as well as their homogeneous distribution inside the porous network.

The synthesis of Ce–TiO_x mixed metal oxides inside the npAu network was based on a sol–gel coating method (Figure 8). In a typical synthesis, npAu was first prepared by the free corrosion method. Subsequently, a Ce–TiO_x mixed metal oxide gel was deposited on npAu disks via the hydrolysis and condensation of TBOT (Ti-tetrabutyl-orthotitanate) and $Ce(NO_3)_3$ in pure ethanol with a low content of concentrated ammonia (0.3vol %). Followed by a thermal treatment process, the mixed metal oxide modified npAu could be obtained and exposed catalytically active form could be obtained after removal of residual groups from the synthesis process.

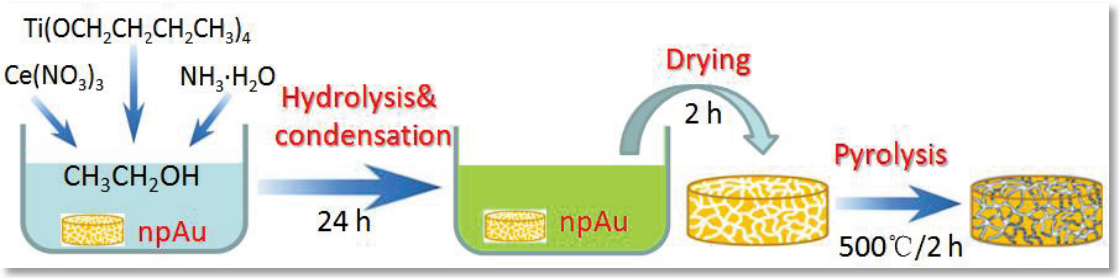

Figure 8. Scheme for the fabrication of titania-ceria mixed oxide coatings inside nanoporous gold.

Similar to the CeO_x/npAu samples, the effect of post deposition annealing on the morphology of the Ce–TiO_x modified npAu was first studied by scanning electron microscopy. Representative cross-sectional scanning electron micrographs of $Ce_1Ti_2O_x$/npAu were chosen to document the morphology of the material. As shown in Figure 9, the ligaments and nanopore channels are homogenously arranged in the bicontinuous 3D network after the annealing treatment. The higher magnification images from the surface and middle part of the sample show no aggregates inside the pores after annealing. The average ligaments size is around 45 ± 2 nm. EDX spectroscopy in different depths along the cross section revealed that the content of Ce is around 2 ± 0.5 atom% and of Ti is around 4 ± 0.5 atom%, consistent with a nominal ratio of the sample corresponding to $Ce_1Ti_2O_x$. These findings demonstrate that the sol–gel method is a very good way to homogeneously grow metal oxide deposits inside the npAu and it provides control over the composition of oxide. At the same time, the tiania–ceria oxides can also effectively stabilize the nano-pores structure up to 500°C.

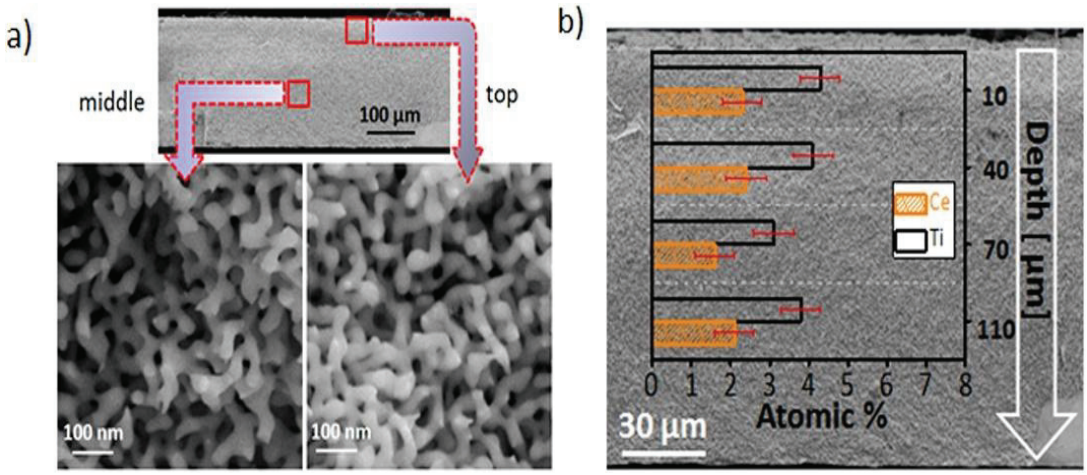

Figure 9. Characterization of titania–ceria modified nanoporous gold. a/b) SEM of a freshly broken cross-section of a $Ce_1Ti_2O_x$/npAu disk (~150 µm thick) sample. The sample was heated to 500°C prior to characterization to demonstrate the structural stability of the material upon heating. a) On the left, a section of the material in the inner part of the material (~75 µm from surface); on the right, a corresponding section close to the outer surface. b) EDX measurement from different depths in the cross sections. (Reproduced from publication II, copyright Royal Society of Chemistry, 2016)

The further structural characterization with transmission electron microscopy (TEM) (Figure 10, $Ce_1Ti_2O_x$/npAu) shows that the gold ligament size is about 40 nm to 50 nm in line with the SEM measurements. The HRTEM characterization of the convex region of ligaments proves that the gold ligaments are covered by small agglomerates which are around 2 nm in size (Figure 10b,d) and clearly exhibiting a crystalline structure. The elemental maps that have been recorded in the energy filtered mode of the TEM (EFTEM) clearly show an enhanced Ce and Ti (Figure 10e) signal at the surfaces of the npAu, where the crystalline particles can also be seen (Figure 10c). This finding confirms that the nanoparticles are composed of Ti and Ce.

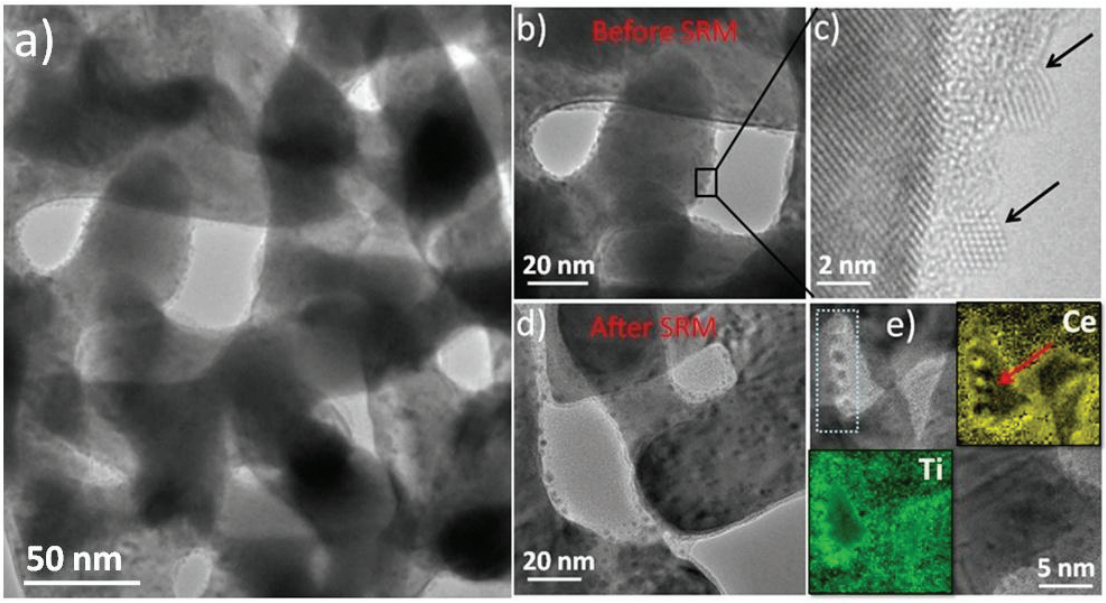

Figure 10. a/b) TEM and c) HRTEM images of nanoporous gold modified by titania–ceria mixed oxides ($Ce_1Ti_2O_x$/npAu) after calcination at 450°C in helium for 2h; the arrow in c) indicates oxide particles on the npAu surface, d/e) TEM and elemental maps of ceria and titania obtained in the EFTEM mode after the catalytic experiments. (Reproduced from publication III, copyright Royal Society of Chemistry, 2017)

4. Interaction of different gases (O_2, CO, H_2O) with CeO_x/npAu, TiO_x/npAu and Ce-TiO_x/npAu

(Relevant papers: I&II)

One of the main interests in this PhD project was to study the effect of the deposition of oxides on npAu on the chemical reactivity of the system. To begin with, we studied the interaction of simple gas molecules, such as CO, O_2, H_2O, with oxide modified npAu. Raman scattering has been used to study the crystallinity and the behavior of oxygen vacancies within the npAu supported metal oxides under different gases conditions.

In the study disks of npAu containing pure CeO_x and TiO_x as well as Ti-CeO_x mixed oxides were first activated at 450°C in N_2/He for 2 h and then broken into 4 pieces (guaranteeing exactly the same starting/preparation conditions) followed by heating to 400 °C under different gas atmospheres for 2 h. Figure 11a shows the Raman spectra of CeO_x on a planar gold/sapphire substrate and on npAu. All spectra show the typical characteristic first-order F_{2g} mode of cubic CeO_2 at around 460 cm^{-1}.[62-63] This mode is attributed to the symmetric stretching mode of the Ce-O_8 vibrational unit.[62, 64-65] As compared to the planar and sapphire substrates, the npAu-supported CeO_x shows an additional broad signal at around 560 cm^{-1}, which can be attributed to a defect-induced mode (D-peak, more details in publication Ⅰ). As indicated in Figure 11b, showing the situation when the sample was exposed to reducing conditions in a CO atmosphere, the D-peak intensity increased. In contrast, when the sample was exposed to an oxygen-or water-containing atmosphere, the D-peak intensity decreased. This result implies that the D-peak intensity indeed relates to the oxygen vacancies in the cerium oxide, which are dynamically responding to the reducing or oxidizing gas atmosphere.[63, 66-68] The finding also indicates that both, oxygen and water, can be dissociated on the catalyst surface, and oxygen atoms can be incorporated into the ceria lattice.

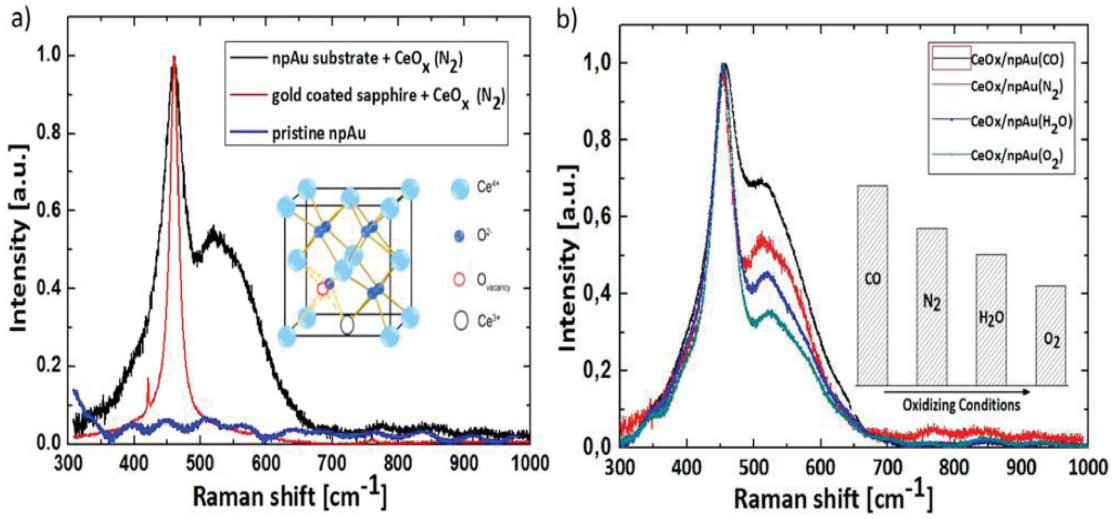

Figure 11. Raman spectra of cerium oxide (@ 785 nm excitation) prepared by thermal decomposition of cerium nitrate. (a) Cerium oxide on a planar gold/sapphire substrate in comparison to cerium oxide on npAu, the baseline is the Raman spectrum of pristine npAu. The small peak at around 425 cm^{-1} (red line) is attributed to the sapphire substrate. Inset shows a schematic representation of cubic fluorite structure of CeO_2. (b) Raman spectra of cerium oxide on npAu. Inset: the bar plot describes the defect peak maximum as a function of the increasingly oxidizing conditions. (Reproduced from publication I, copyright American Chemical Society, 2014)

In addition, the treatment under different gas atmospheres has an impact on the formation of the crystalline phase. After exposing the TiO_x/npAu sample to an O_2 atmosphere, the peaks (B_{1g}, A_{1g}, E_g) due to the crystalline phase grow in intensity and the broad peak at 695 ± 3 cm^{-1} due to amorphous titania disappears(Figure 12a).[69-71] This implies that the crystallinity of titania increases after adding oxygen to the defects, i.e. oxygen vacancy sites, of the initially amorphous titania. In contrast, the treatment in a H_2O atmosphere has a negligible influence on the sample with respect to the intensity of both, the amorphous peak (695 ± 3 cm^{-1}) and the anatase peaks (B_{1g}, A_{1g}, E_g). This finding indicates that H_2O is more difficult to dissociate than O_2 on the TiO_x/npAu surface. In addition, after the treatment in a reducing CO atmosphere most of the titania is transformed into an amorphous state, implying the introduction of defects in the oxide by removing lattice oxygen.

From the Raman spectra of $Ce_1Ti_2O_x$/npAu and $Ce_1Ti_3O_x$/npAu (Figure 12b and c) we can see that the typical Raman modes of anatase TiO_2 and cubic CeO_2 (~460 cm^{-1})

are not present, indicating a low content of crystalline phases of both TiO_2 and CeO_2. After oxidizing with O_2 or H_2O, however, a very broad peak centered at around 710 cm^{-1} becomes noticeable. This indicates the formation of titanates and cerium titanates, respectively.[64, 72-74] In the study we find the formation of cerium titanates after treatment of the catalysts in water or oxygen atmosphere, while no changes can be observed when heating in an inert gas atmosphere (Figure 12b and c). Similar to CeO_x/npAu sample, this observation indicates that water and oxygen are dissociated on the catalyst surface and oxygen atoms are incorporated into the crystal lattice. In addition, further treatment of an oxidized sample in a CO containing atmosphere reveals that the amorphous titania peak shows up again (Figure 13a) and the cerium titanates-peak's intensity are reduced (Figure 13b), indicating that oxygen can be dynamically stored in the lattice of the npAu supported oxides.

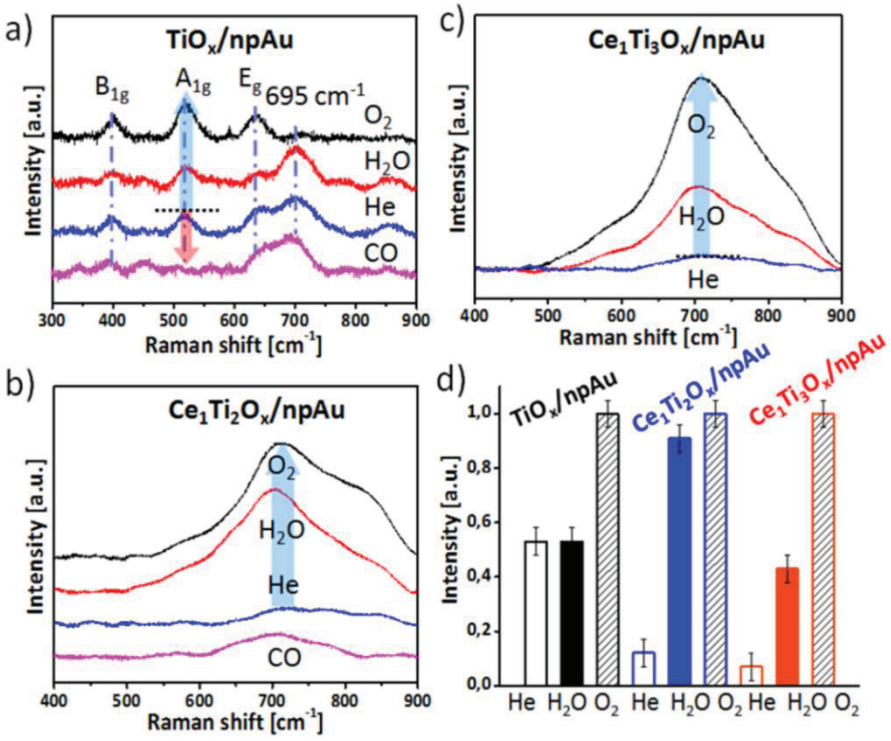

Figure 12. Raman spectra of (a) TiO_x/npAu and (b) $Ce_1Ti_2O_x$/npAu (c) $Ce_1Ti_3O_x$/npAu. The samples were first thermally treated at 450°C in He for 2 h, and then broken into several pieces and heated under different gas atmospheres (CO, H_2O, and O_2 with 13, 30, and 13 vol%, respectively, in He as carrier at 400 °C for 2 h). d) Evolution of the intensity of the A_{1g} (TiO_x/npAu) and the Raman band at ~710 cm^{-1} (Ce-TiO_x/npAu) after heating in He, H_2O and O_2 containing atmosphere. (Reproduced from publication II, copyright Royal Society of Chemistry, 2016)

The peak intensities were compared after heating in different gas atmospheres (A_{1g}

for the TiO_2/npAu, the band at ~710 cm^{-1} for the Ce–TiO_x/npAu samples) in order to semi-quantitatively evaluate the changes from the amorphous state to the more crystalline state. All samples show increased crystallinity upon heating in O_2 atmosphere, whereas after heating in a H_2O containing atmosphere (Figure 12d), the samples show quite significant differences. The $Ce_1Ti_2O_x$/npAu sample shows the most prominent changes, which are more than twice as large as compared to all other samples. This finding demonstrates that the $Ce_1Ti_2O_x$/npAu sample shows the highest activity for dissociation of H_2O among the three catalysts.

To conclude, the addition of oxides to npAu obviously enhances the chemical reactivity of the system and makes it more reactive for the dissociation of molecules, such as O_2 and H_2O.

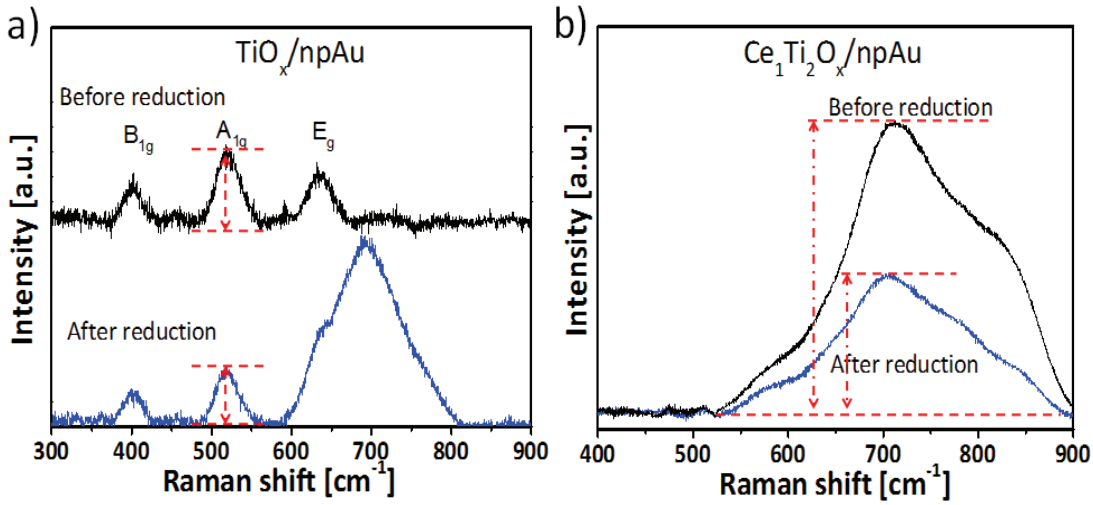

Figure 13. Raman spectra of a) TiO_x/npAu and b) $Ce_1Ti_2O_x$/npAu before and after CO reduction. After treating the sample in an O_2 atmosphere at 400°C for 2h, the sample was broken into two pieces. Then one part of the oxidized sample was reduced under CO atmosphere at 400°C for 2h. (Reproduced from publication II, copyright Royal Society of Chemistry, 2016)

5. The Water-Gas Shift on CeO_x/npAu, TiO_x/npAu and Ce-TiO_x/npAu: Optimizing the Active Sites for the Catalytic Process

(Relevant papers: I&II)

The WGS reaction is an important catalytic process for the production of clean hydrogen. In the last decades there has been an increased demand for novel types of water-gas shift (WGS) catalysts in the context of mobile and green energy harvesting such as in fuel cells application.[24, 75] Recently, both Au/CeO_2 and CeO_2/Au(111) materials were reported to be very promising catalysts for the lower-temperature WGS reaction.[24, 44] The UHV study from Rodriguez et al. indicates that the high performance of CeO_2/Au(111) catalysts in the WGS requires the presence of both oxide and metal.[44] The oxide plays an important role in facilitating the dissociation of water because Au itself cannot perform this reaction. This is also in line with our studies on the oxide functionalized npAu. It is known that npAu itself is a very active catalyst for oxidation of carbon monoxide which is based on the dissociation of molecular oxygen. The current study points to the fact that the oxide functionalized npAu can efficiently dissociate both molecular oxygen and water, and now the question arises if the material could also catalyze the water based oxidation reaction such as the WGS reaction and steam reforming of methanol?

To answer this question, we first studied CeO_x functionalized npAu for the WGS reaction. As shown in Figure 14a and b, the deposition of CeO_x on npAu yield surfaces with high catalytic activity for both the WGSR and CO oxidation. Starting at about 135°C the first catalytic conversion of H_2O and CO to CO_2 was observed (Figure 14a). The catalytic activity increased strongly with temperature. The Arrhenius plot reveals an apparent activation barrier E_a of around 31 kJ/mol (Figure 14a). This value is comparable to the result from Fu et al., who measured an E_a of

about 37 kJ/mol with a CeO_2-supported Au nanoparticles catalyst.[76] In addition, the catalyst displayed a good long-term stability; after three test cycles, a total of 15 h, the CeO_x/npAu sample only lost about 10% activity at 535°C. As anticipated, the activity for CO oxidation is much higher even at lower temperatures as compared to WGSR; for example, the formation of CO_2 using O_2 sets in at 60°C (Figure 14b). A similar conversion was detected only at 240°C when using water as the oxidant. It is known that the O-O bond (146 kcal/mol) has a much lower energy than O-H bond (467 kcal/mol).(Libretext chemistry library) Therefore, the high activity for oxidation by O_2 at much lower temperatures can be attributed to faster/easier activation of molecular oxygen of the CeO_x/npAu catalyst surface.

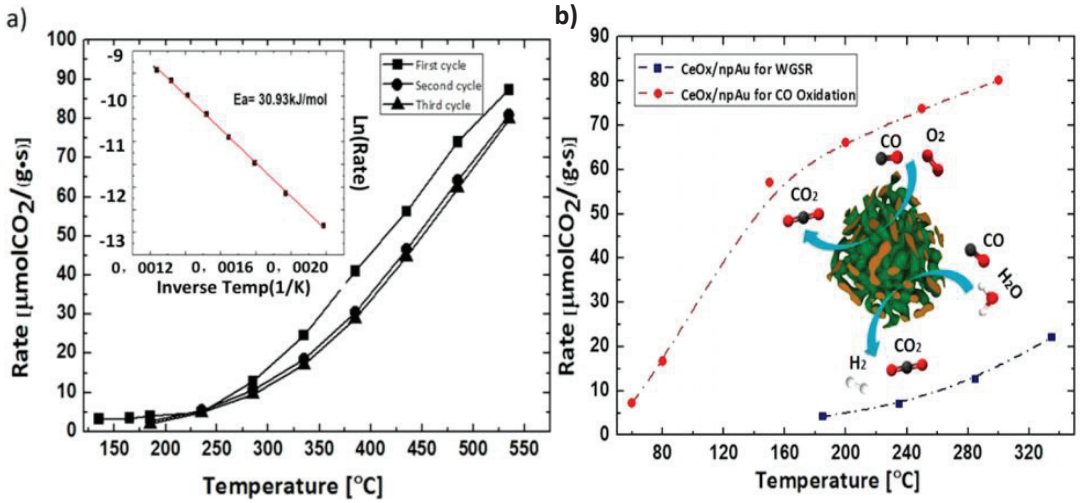

Figure 14. WGS activity ($CO + H_2O \rightarrow CO_2 + H_2$): (a) using a 150 μm thick free-standing disk of CeO_x/npAu (4.2 vol% CO, 16.0 vol% H_2O in N_2, total gas flow 43.8 mL/min, M_{catal} = 5.1 mg, space velocity 515 000 mL $h^{-1}g^{-1}_{cat}$). The inset shows an Arrhenius plot of the data revealing an apparent activation energy of 31 kJ/mol. (b) Comparison of the reaction rate for oxidation of CO by H_2O (lower line) or O_2 (upper line) using a CeO_x/npAu catalyst (for CO oxidation 2.9 vol % CO, 47.0 vol % O_2 in N_2, m_{catal} 4.4 mg; for WGS reaction 4.2 vol % CO, H_2O 16.0 vol % in N_2. m_{catal}= 4.8 mg). (Reproduced from publication I, copyright American Chemical Society, 2014)

Photoelectronspectroscopic (PES) characterization of samples prior to and after catalytic testing revealed that all the samples contained a high concentration of Ce^{3+} of about 65-75% (Figure 15). This observation suggests that under the chosen annealing temperatures (>235°C) and under a protecting inert gas atmosphere (N_2/He) the Ce^{3+} is only partially oxidized to Ce^{4+}. To be mentioned, the defect concentration

(Ce^{3+}) stays quite constant or even slightly increases after the WGS reaction. This can be due to the synergy effect between the npAu and the ceria deposits which helps maintaining these defects[44, 46, 77-78] and, thus, the catalytic activity even under oxidizing conditions.

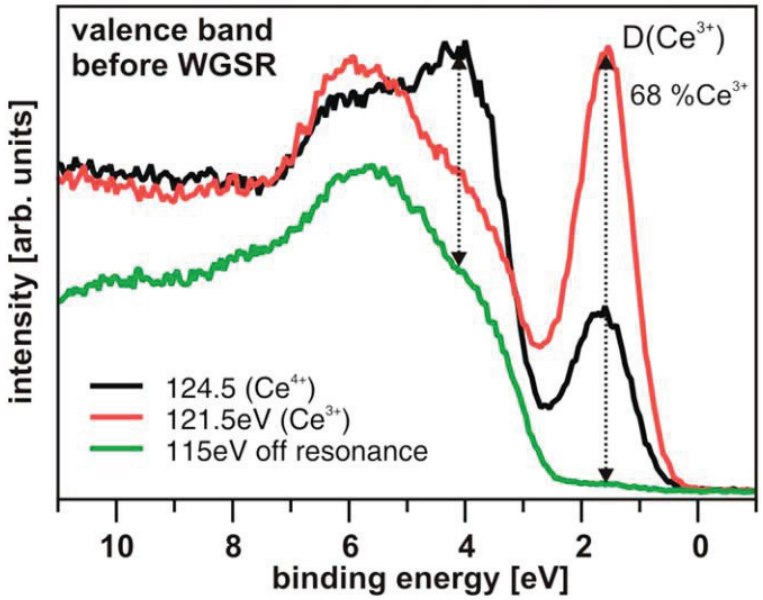

Figure 15. Resonant photoemission of Ce^{3+}/Ce^{4+} on the CeO_x/npAu film catalysts at the valence band. (Reproduced from publication I, copyright American Chemical Society, 2014)

This first study shows that CeO_x functionalized npAu holds great promise for WGSR applications at ambient pressure over a wide temperature range. Spectroscopic characterization by photoemission reveals that the cerium oxide is rich in defects (Ce^{3+}) in combination with npAu. (pure ceria contains around 18% Ce^{3+}).[79] Such surface defect sites facilitate the dissociation of water, and thus promote this reaction.

To test if npAu functionalized with the mixed oxides of CeO_2 and TiO_2 show higher activity, we compared the performance of Ce–TiO_x/npAu to npAu functionalized with pure TiO_2 as well as pure CeO_2 with respect to WGSR. As can be seen in Figure 16a start of the catalytic conversion of water and CO can be observed over all the catalysts at a temperature of 200°C. Also, the catalytic activity for all the catalysts increases in an exponential fashion with temperature. TiO_x/npAu exhibits the lowest activity in the whole temperature range. The bar plot (Figure 16b) at 300°C for all samples reveals that the addition of even small amounts of Ce to TiO_2 results in an increased activity

by ~30%. The $Ce_1Ti_2O_x$/npAu sample shows the highest activity with a reaction rate of 27 µmol CO_2 $g^{-1}s^{-1}$, which is around 3 times of the values reported by Si et al. (9.3 µmol CO_2 $g^{-1}s^{-1}$ at 300°C) for Au–Ti–CeO_2 powder catalysts.[80] The corresponding TOF is ~0.3 s^{-1}, calculated by assuming a specific surface area of the npAu catalyst of around 4 m^2g^{-1}. However, when taking mass transport and coverage of the surface by oxide particles into account, the calculated TOF might even be higher.[18, 43]

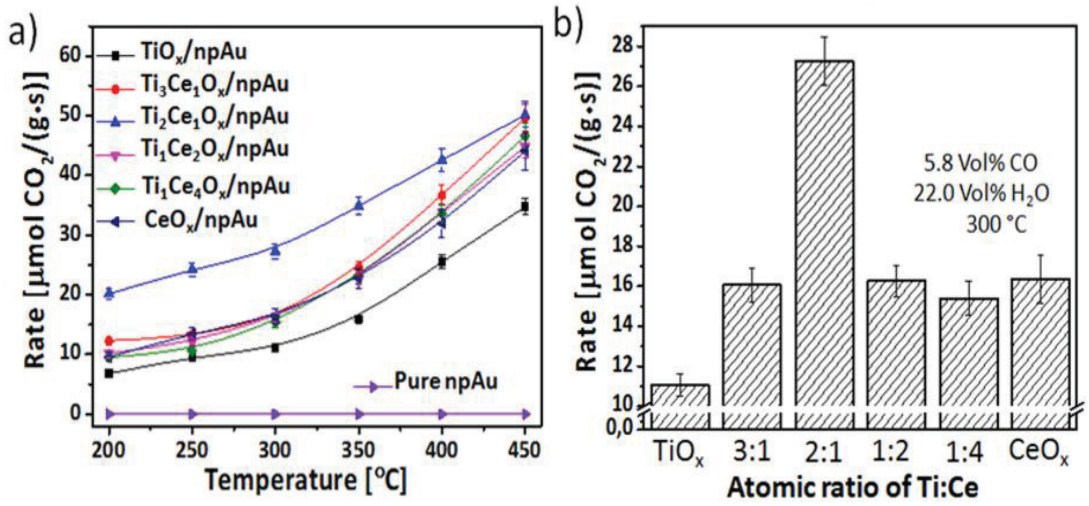

Figure 16. WGS activity (CO + H_2O → CO_2 +H_2): a) comparison of the reaction rate of different binary Ti–CeO_x and TiO_2 or CeO_2 single oxide functionalized npAu samples (5.8 vol% CO, 22.0 vol% H_2O in He, total gas flow of 32 mL min^{-1}, m_{catal} = 6.0 ± 0.2 mg, space velocity 320 000 $mLh^{-1}g_{cat}^{-1}$). b) The bar plot for the catalysts is based on the reaction rates measured at 300°C (each measurement was repeated at least 4 times with different catalysts). (Reproduced from publication II, copyright Royal Society of Chemistry, 2016)

6. The Steam reforming of methanol over CeO_x/npAu, TiO_x/npAu and Ce-TiO_x/npAu

(Relevant paper: III)

Besides the water gas shift reaction another important approach for the production of hydrogen is steam reforming of methanol (SRM).[81-84] It provides an effective way to leverage the existing infrastructure in fuel storage and dispensing,[85-87] owing to the liquid nature of methanol at atmospheric pressure and other advantageous properties such as a high H/C ratio, no sulfur contaminations, and easy synthesis from renewable and fossil fuels.[88-93] The mechanism of SRM is still being debated, even for the extensively studied Cu- and Pd/ZnO-based catalysts.[85, 91, 94-101] From the chemical equation we can see that water adsorption and dissociation should also be involved in the catalytic process. The previous study already demonstrates that the oxides functionalized npAu are highly active for the dissociation of H_2O in WGSR and we know that npAu is also highly active for the selective oxidation of methanol with molecular O_2. So, theoretically, the oxide functionalized npAu might also be able to catalyze the SRM reaction. In the following section we have examined the $Ce_1Ti_2O_x$/npAu, CeO_x/npAu and TiO_x/npAu system as SRM catalyst, and investigated the dependence of the activity and selectivity on the temperature and on the nature of the oxide deposits.[102]

Figure 17 reveals the different activities of the three samples for the SRM reaction. Obviously, the CeO_x-modified npAu shows the highest reactivity, followed by $Ce_1Ti_2O_x$/npAu, and TiO_x/npAu, which exhibits the lowest activity in the whole temperature range (for more details see publication Ⅲ). A control experiment with pure npAu or pure metal oxides demonstrates that the reforming of methanol is negligible on these systems. In addition, all three catalysts exhibit high CO_2 selectivity (～100 %) below 350°C (Figure 17b) and the CO concentration is below

the detection limit. After increasing the temperature above 350°C, CO can be detected indicating a lower CO_2 selectivity at high temperatures.

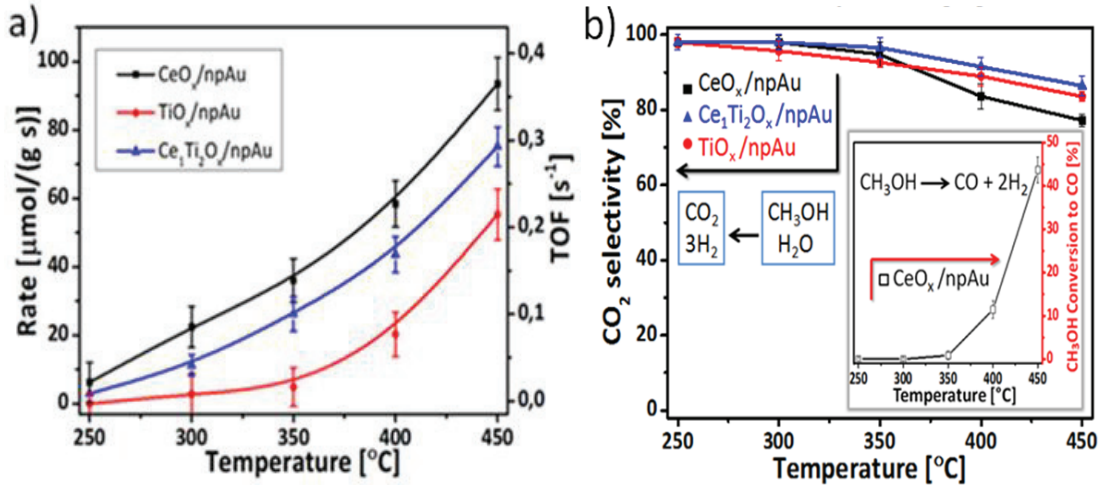

Figure 17. (a) CH_3OH conversion rate to CO_2 in steady-state tests of SRM over $Ce_1Ti_2O_x$/npAu, CeO_x/npAu and TiO_x/npAu; (b) CO_2 selectivity (%) in steady-state tests of SRM over CeO_x/npAu (solid squares), $Ce_1Ti_2O_x$/npAu (solid triangles), TiO_x/npAu (solid circles). The inset in Fig. 17b shows the dehydrogenation of CH_3OH to CO in the absence of H_2O over CeO_x/npAu (hollow squares). (Reproduced from publication III, copyright Royal Society of Chemistry, 2017)

7. Hydroxyl groups (OH) on the surface of CeO_x/npAu and Ce-TiO_x/npAu: Origins of the catalytic activity of oxide functionalized nanoporous gold

(Relevant papers: I&III)

Hydroxyl groups on oxide surfaces are the key species in lots of surface and interface reactions, because they determine the acid-base chemistry and catalysis properties of the oxide materials.[103] They are reported to be involved in many catalytic reactions, such as CO oxidation and alcohol oxidation, as also catalyzed by oxide-supported Au particles.[104] The presence of hydroxyl groups can promote the reaction rate even by several orders of magnitude. For example, Date et al. studied the influence of H_2O on CO oxidation activity over Au/SiO_2 at 273 K and found that an increase of the water concentration from 0.3 to 200 ppm can result in an increase of the reaction rate by 2 orders of magnitude.[104] My colleague Wittstock observed similar results for the on the npAu catalyzed CO oxidation; just by adding 0.01 vol% water to the gas stream the conversion of CO was increased by about 100 %.[105] It is believed that during the reaction a hydroxyl species can directly react with CO to form COOH, which eventually decomposes to CO_2.

Both UHV studies and DFT calculations point to the fact that there is only very weak bonding between water and a clean Au surface.[18, 104] In contrast to Au, oxides especially those with redox properties, have a relatively high ability for water adsorption and further dissociation into active hydroxyl groups.[18] Therefore, the addition of titania/ceria on the npAu surface facilitates the breaking of O-H bonds in the dissociation of water ($H_2O \rightarrow OH + H$). We have discovered that different oxide functionalized npAu catalysts exhibit different catalytic activities. The understanding of the different activities requires knowledge of their surface properties, especially those related to the hydroxyl groups. Photoelectron spectroscopy and diffuse reflectance infrared spectroscopy (DRIFT) have been used to study the surface

properties of samples for the WGSR and SRM.

Figure 18 shows the XPS spectra in the O1s region of the CeO_x/npAu catalyst before and after the WGS reaction. The lattice O signal from CeO_x is present in both spectra at 529.8 ± 0.15 eV. Another feature at around 532 ± 0.15 eV is attributed to OH groups on the catalyst surface.[39] After WGS reaction there is an obvious increase of the OH/O ratio from 1.1 to 2.2. In addition, a further feature at around 531 ± 0.15 eV is related to a cerium hydroxide $Ce(OH)_x$ phase. According to the literature, the key step for the WGS reaction is the adsorption and dissociation of water into adsorbed OH and H.[44] The observed increase of OH/O ratio and the rise of the $Ce(OH)_x$ peak after the WGS reaction can, thus, be attributed to the dissociation of water on CeO_x.

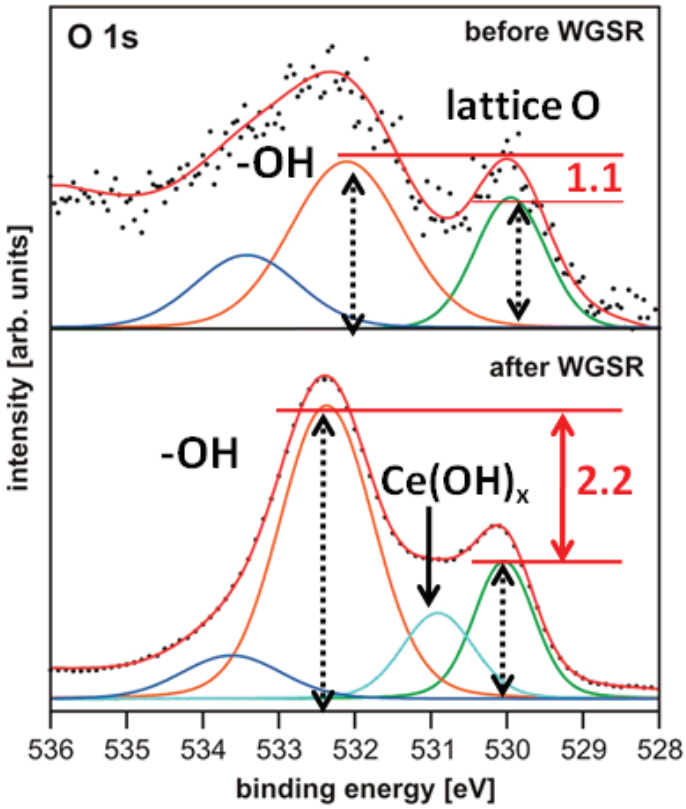

Figure 18. Photoemission features in the O 1s region on the CeO_x/npAu film catalysts before (upper section) and after WGS reaction (lower section). (Reproduced from publication I, copyright American Chemical Society, 2014)

To investigate the adsorption and evolution of CH_3OH and $CH_3OH + H_2O$ on the oxides/npAu surface, we performed in-situ studies of these catalysts by diffuse

reflection FTIR spectroscopy (DRIFTS). A set of experiments was recorded at temperatures between about –35°C and 20°C (low temperature regime). Such low temperatures are well below the desorption temperature of methanol and reaction products on the oxide surfaces, such as CeO_2 (>500 K) as the initial reaction products can accumulate on the surface rather than desorb or further react.[106, 107]

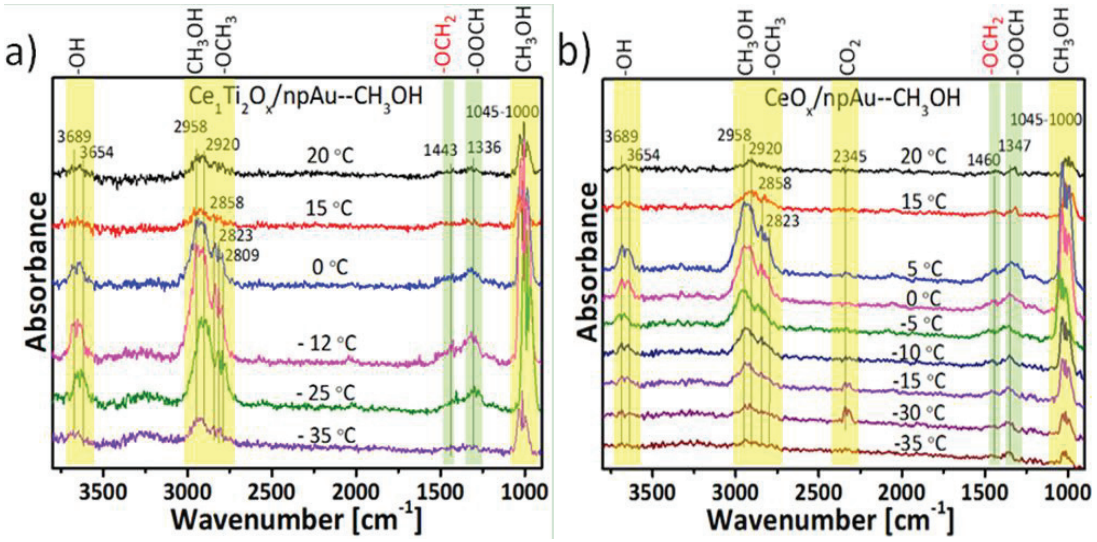

Figure 19. In-situ DRIFT spectra under He atmosphere (30 mL/min) for (a) $Ce_1Ti_2O_x$/npAu and (b) CeO_x/npAu catalysts after exposure to CH_3OH at - 35°C. (Reproduced from publication III, copyright Royal Society of Chemistry, 2017)

From the low temperature in-situ DRIFT spectra we learn that the exposure of oxide functionalized npAu to CH_3OH results in the formation of surface-bonded methoxy (CH_3O*) (bands at 2920 and 2823cm^{-1}, Figure 19).[97] The observation of species like formaldehyde (H_2CO*) and formate (HCOO*) can be attributed to the dehydrogenation/oxidation of methoxy.[97] Moreover, OH groups (bands at 3689 and 3654 cm^{-1}) can be observed which indicate the reaction of hydrogen with surface oxygen atoms. After increasing the temperature to 20°C all the absorbed species can not persist on the surface.

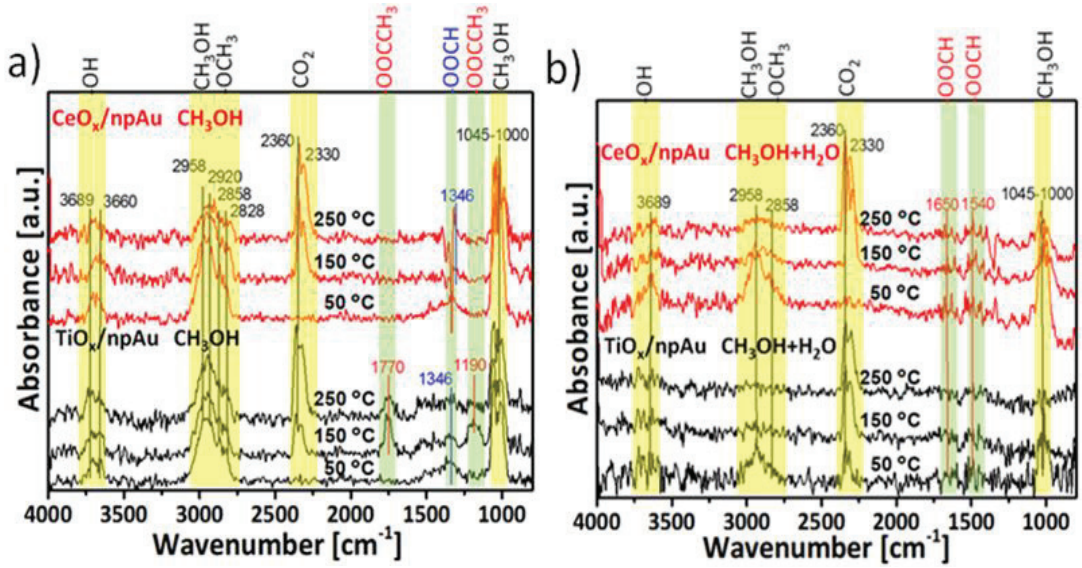

Figure 20. Steady state flow in-situ DRIFT spectra recorded for CeO_x/npAu and TiO_x/npAu catalysts. (a) CH_3OH (13 vol%) and (b) mixture of CH_3OH (1.3 vol%) and H_2O (2.0 vol%) at temperatures starting at 50°C to 250°C. (Reproduced from publication III, copyright Royal Society of Chemistry, 2017)

Following the low temperature in-situ DRIFT experiments, a steady state flow in-situ FTIR experiments (50-250°C) were conducted by exposing CeO_x/npAu and TiO_x/npAu to methanol or mixtures of methanol and water. No formaldehyde is observed ($\delta(CH_2)$ at 1443 cm^{-1}) in Figure 20, which is due to the comparably weak bonding ability of the species, so that low surface concentration result under SRM conditons.[100, 108] Starting at 150°C, two new bands are present on the TiO_2/npAu surface (Figure 20a), indicating the formation of methyl formate (1770 cm^{-1} and 1190 cm^{-1}). At the same time, two negative bands (1400 and 1338 cm^{-1}) appear for the CeO_x/npAu sample, which can be attributed to the desorption/consumption of surface –OH group. After exposing the sample to a mixed gas of methanol and H_2O, all the spectra show obvious changes: the intensity of methoxy decreases, surface species like formate and methyl formate disappear (Figure 20b), and two small bands (1650 cm^{-1} and 1540 cm^{-1}) indicative of bidentate formate become obvious. The observation of the bidentate formate is related to the low activities of the species with respect to further dehydrogenation.[97]

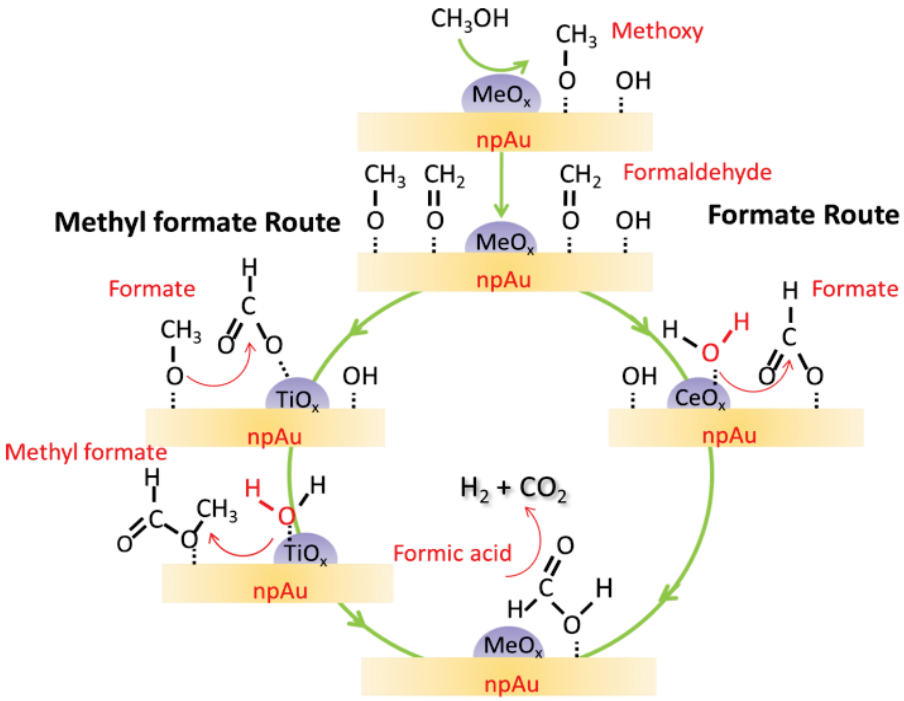

Figure 21. Mechanism of steam reforming of methanol on oxides functionalized npAu. (Reproduced from publication III, copyright Royal Society of Chemistry, 2017)

Two different reaction mechanisms have been proposed for the SRM.[97, 100, 108] The first step is the same for both mechanisms, that is the deprotonation of methanol and the formation of surface methoxy, which is subsequently dehydrogenated to formaldehyde. (Figure 21) However, based on our research we find that the presence of reactive hydroxyl on the catalyst surface will further regulate the following reaction steps. The amount of reactive hydroxyl groups will control whether formaldehyde is completely dehydrogenated to CO, or reacts with an adjacent methoxy group forming methyl formate, or reacts with extra OH forming formic acid. In turn, by detecting intermediates on the catalyst surface we can also draw conclusions about the availability of reactive OH groups on the catalyst surface.

The formate pathway

$$CH_3OH \rightarrow CH_3O^* + H^* \rightarrow H_2CO^* + 2H^*$$

$$O^*/OH^* + H_2CO^* \rightarrow HCOO^* + H^*/H_2$$

$$HCOO^* \rightarrow CO_2 + H^*$$

Methyl formate pathway

$$CH_3OH \rightarrow CH_3O^* + H^* \rightarrow H_2CO^* + 2H^*$$

$$CH_3O^* + H_2CO^* \rightarrow HCOOCH_3 + H^*$$

$$HCOOCH_3 + H_2O \rightarrow HCOOH + CH_3OH$$

$$HCOO^* \rightarrow CO_2 + H^*$$

The DRIFTS study shows that no CO is observed on the catalyst surface. We can therefore conclude that all oxide/npAu catalysts provide sufficient concentrations of OH groups to prevent complete dehydrogenation of formaldehyde to CO. The formation of methyl formate on the TiO_2/npAu surface suggests that it is less active for the dissociation of water than the CeO_x/npAu and $Ce_1Ti_2O_x$/npAu. The finding is also in line with previous studies on the water gas shift reaction.[41]

In summary, the activity of the oxide functionalized npAu catalysts is linked to the availability of reactive OH groups on the catalyst surface. The presence of oxides on the npAu support is a key factor in determining the catalytic activity because npAu itself is not able to break the O-H bond in water. The coupling of npAu to ceria/titania produces a bifunctional metal-oxide interface that is able to dissociate water, which opens a possibility for tuning the properties of npAu for the future applications in heterogeneous catalysis.

8. Summary and outlook

The fabrication and applications of metal oxide-functionalized npAu was intensivly studied in this work with the emphasis on the control of the composition and distribution of the metal oxides, clarifying the role of the oxide deposits in catalytic applications, such as the WGSR and SRM, and illustrating the reaction mechanism for the SRM reaction.

The modification of nanoporous gold with different metal oxides was first investigated. After deposition of ceria, temperature-induced coarsening of gold ligaments could be effectively suppressed even at temperatures of more than 500°C. However, the inhomogeneous distribution of the precursor solution in the npAu samples caused partially coarsening of the structure. To overcome this problem and improve the WGSR catalytic activity, a simple and versatile sol-gel coating method was developed. The SEM and TEM characterization showed that TiO_x and mixed Ce-TiO_x can be homogenously deposited onto npAu and the composition can be well controlled.

To further shed light on the effect of depositing oxides on npAu on the chemical reactivity of the system, the interaction of simple gas molecules (CO, O_2, H_2O) with the oxide modified npAu was studied with Raman scattering. The formation of oxygen vacancies could be detected after heating in reducing atmospheres like CO. Oxygen and water could be dissociated on the catalyst surface, and oxygen atoms could be dynamically stored in the lattices of the npAu supported oxides.

In addition, the catalytic activity of inverse oxide functionalized npAu catalysts for the WGSR was investigated. The first study showed that CeO_x functionalized npAu holds great promise for WGSR applications at ambient pressure over a wide temperature range. The X-ray photoelectron spectroscopy revealed that the cerium oxide was rich in defects (Ce^{3+}) after the preparation, which facilitated the dissociation of water, and thus promoted this reaction. By comparing the activity of different catalysts, it was found that the composition of the oxide played a key role,

the sample with a Ti :Ce ratio of 2 : 1 showed an increase in activity by over 100%. This study showed that the control over the composition of the oxide can provide an ideal way for tuning the activity of the catalyst.

Moreover, metal oxide-functionalized npAu as a new type of catalyst for the methanol steam reforming reaction was investigated. The catalytic activities of $Ce_1Ti_2O_x$/npAu, CeO_x/npAu and TiO_x/npAu were compared. Notably, ceria and mixed oxide functionalized npAu showed excellent low-temperature catalytic activity and selectivity for the SRM within a broad temperature (250-450°C) window.

Last but not least, the impact of surface hydroxyl groups on the material properties was investigated. The availability of reactive OH groups on the catalyst surface determined the activity of the catalyst and had an influence on the reaction mechanism. The coupling of npAu to different oxide provides a new way to tuning the surface properties of npAu for broader applications in heterogeneous catalysis.

In future work, it will be interesting to extend the application of the catalysts in this work to other catalytic reactions such as CO_2 hydrogenation to methanol. Recently, Rodriguez and Chen et al. showed that the interaction of Au with CeO_x/TiO_2 at the interface can lead to a charge redistribution in the metal, the resulting polarization of the metal−oxide interface can promote both, CO_2 adsorption and activation.[109] Furthermore, the sol−gel strategy for coating npAu started in this work can represent a blueprint for the rational design and controllable synthesis of other useful npAu-based materials.

9. Experimental

9.1 Flow Reactor Studies

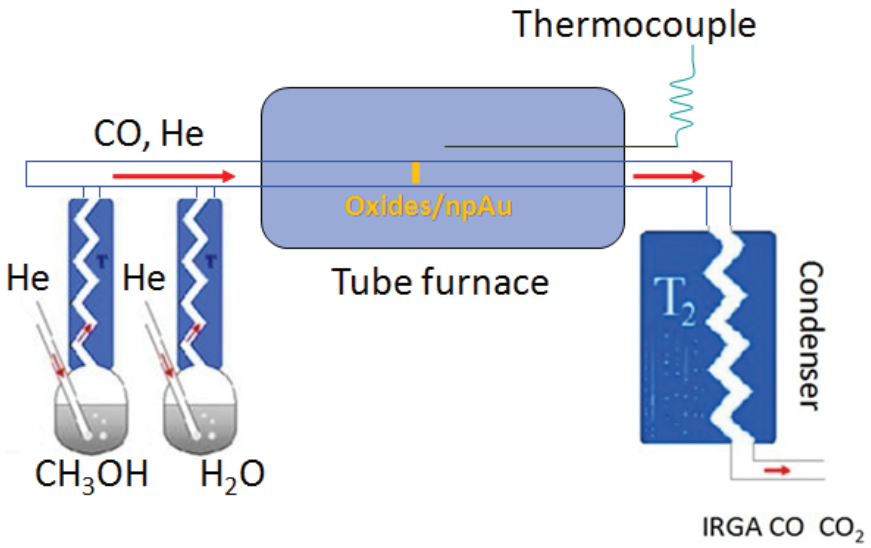

Figure 22. Schematic drawing of the experimental setup for measuring the catalytic conversion of CO and methanol, respectively. The content of methanol or water in the feed gases were adjusted by their vapour pressure and the flow rate of the carrier gas (He). The MO_x/npAu catalyst was placed in the middle part of the quartz tube and fixed with quartz wool. An ice condenser was installed at the reactor exit in order to remove the moisture in gas stream. The composition of the gas stream was investigated by IR analyzers (URAS 3G, Hartmann and Braun).

Figure 23. Experimental setup for measuring the catalytic performance of MeO_x/npAu. Flow and composition of gases were precisely controlled via mass flow controllers (upper left). The stream of gases was guided towards the reactor through a steel pipe, the outside of the pipe was wrapped with heating tape and covered with aluminum foil. For experiments using e.g. H_2O or methanol an additional He stream was guided through a saturator system to precisely adjust the content of the particular liquid in the gas phase.

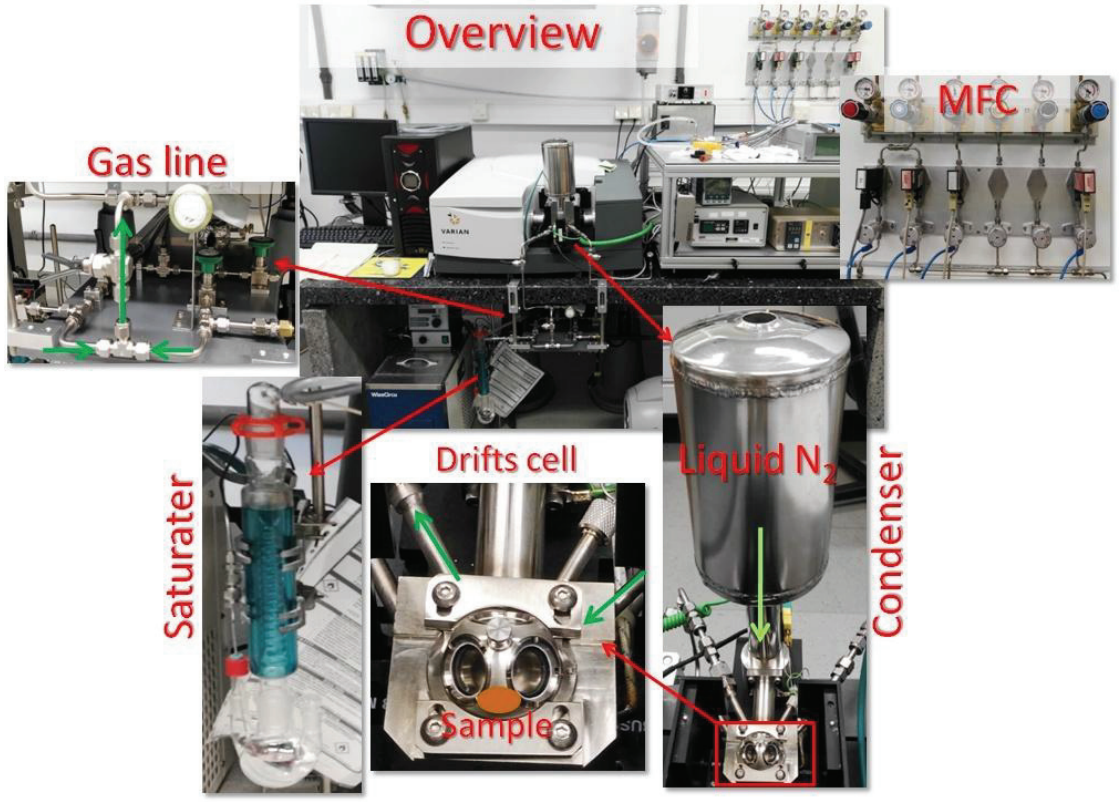

Figure 24. Photographs of the diffuse-reflectance FTIR geometry (DRIFT) experimental setup for investigating the mechanism of steam reforming of methanol with different MeO_x/npAu catalysts.

9.2 Characterization

SEM

The cross-sectional scanning micrographs were collected with a ZEISS SUPRA 40 using a SE2 detector and an accelerating voltage of 15 kV. Electron dispersive x-ray spectroscopy (EDX, with spatial resolution/"mapping") was performed using a Bruker XFlash 6130 detector. The average diameters of the Au ligaments were determined by measuring the size of 60 ligaments. The deviation of the EDX data is due to system errors which come from the instrument itself.

TEM

TEM images were recorded in conventional bright field TEM mode using parallel illumination. All measurements were performed with a FEI Titan 80/300 TEM/STEM

equipped with an aberration corrector for the imaging system operated at 300 kV. Preparation of the TEM sample was performed with a focused ion beam (FIB) using a FEI Nova 200 FIB.

Photoemission Spectroscopy

The PES data were acquired at the undulator beamline i411 housing a SCIENTA SES-200 hemispherical analyzer at the Swedish synchrotron radiation facility MAX-IV Laboratory. The samples were mounted using stainless steel clips and the Au 4f signal of a gold piece and the residual Au 4f signal of the coated npAu samples, respectively, were used for binding energy calibration. Resonant photoemission at the Ce NIV,V edge, thus exploiting the 4d-4f transition, was used to determine the ratio of the resonant enhancement factors $D(Ce^{3+})/D(Ce^{4+})$ in the valence band spectra measured at 124.5 eV (Ce^{4+} resonance), 121.5 eV (Ce^{3+} resonance) and 115 eV (off resonance) photon energy, respectively. From that ratio the Ce^{3+} concentration at the very surface can be determined as shown in refs 77 and 78. Uncertainties are added to our evaluation by the presence of surface species (C−, −OH), which also contribute to the VB spectra. Thus, we consider the percentage of Ce^{3+} presented to be accurate by about ±5%.

Raman spectroscopy

The Raman spectra were performed at room-temperature with a Lab Ram ARAMIS (Horiba JobinYvon) Micro-Raman spectrometer which is equipped with a laser working at 785 nm and less than 20 mW. The use of a 50× objective (Olympus) with a numerical aperture of 0.75 provides a focus spot of about 1.3 μm in diameter when closing the confocal hole to 200 μm. Raman spectra were collected in the range of 80 cm^{-1} to 1000 cm^{-1} with a spectral resolution of approximately 1.0 cm^{-1} using a grating of 1800 grooves per mm and a thermoelectrically-cooled CCD detector (Synapse, 1024 × 256 pixels).

In Situ DRIFTS Measurements

In situ Infrared (IR) spectroscopy measurements were conducted in

diffuse-reflectance geometry (DRIFTs) with a Varian-670FT-IR spectrometer equipped with a liquid nitrogen cooled MCT detector. The IR-cell and reaction chamber, respectively, are connected to an external liquid nitrogen cooling system, which allows the cooling of the IR-cell to about -150 °C (Harrick Scientific Products). In a typical experiment, the as prepared npAu disk catalysts (5 mm in diameter) was placed on a temperature-controlled sample holder in the IR-cell. Prior to experiments the sample was in situ heated in He at 300°C for 90 min, in order to remove the residual groups from the precursor and to obtain the metal oxides. After flushing in He for 60 min and cooling to room temperature, the first spectrum was recorded and used as a background reference for all subsequent experiments with this particular catalyst. All spectra shown were recorded with a resolution of 4 cm^{-1} in absorption mode. After exposure to a certain gas mixture the samples were kept at stagnant temperature for 15 min to achieve equilibrium conditions before collecting the spectrum. For pure CH_3OH DRIFTS, the CH_3OH was introduced by passing He through a bubbler (20°C), filled with CH_3OH at a total flow of 30 mL/min. For CH_3OH and H_2O mixed gases, a gas mixture of methanol and water (CH_3OH 10 mol%) was generated by flowing pure helium at 20°C through a bubbler filled with methanol and water, resulting in a molar ratio of 1:1.5 at a total flow of 30 mL/min in SRM.

10. References

1. Zhen Ma, S. D., Heterogeneous Gold Catalysts and Catalysis_Preface. *Royal Society of Chemistry* **2014,** *RSC Catalysis Series No. 18*, P005-P007.
2. Hutchings, G. J., Heterogeneous catalysts—discovery and design. *J. Mater. Chem.* **2009,** *19* (9), 1222-1235.
3. Bravo-Suárez, J. J.; Chaudhari, R. V.; Subramaniam, B., Design of Heterogeneous Catalysts for Fuels and Chemicals Processing: An Overview. **2013,** *1132*, 3-68.
4. Haruta, M., Catalysis of gold nanoparticles deposited on metal oxides. *CATTECH* **2002,** *6* (3), 102-115.
5. Johnston, P.; Carthey, N.; Hutchings, G. J., Discovery, Development, and Commercialization of Gold Catalysts for Acetylene Hydrochlorination. *Journal of the American Chemical Society* **2015,** *137* (46), 14548-57.
6. Masatake Haruta, T. K., Hiroshi Sano, Nobumasa Yamada, Novel Gold Catalysts for the Oxidation of Carbon Monoxide at a Temperature far Below 0°C. *Chem. Lett.* **1987**, 405-408.
7. Biener, J.; Biener, M. M.; Madix, R. J.; Friend, C. M., Nanoporous Gold: Understanding the Origin of the Reactivity of a 21st Century Catalyst Made by Pre-Columbian Technology. *ACS Catalysis* **2015,** *5* (11), 6263-6270.
8. Wittstock, A.; Wichmann, A.; Bäumer, M., Nanoporous Gold as a Platform for a Building Block Catalyst. *ACS Catalysis* **2012,** *2* (10), 2199-2215.
9. Zielasek, V.; Jurgens, B.; Schulz, C.; Biener, J.; Biener, M. M.; Hamza, A. V.; Baumer, M., Gold catalysts: nanoporous gold foams. *Angewandte Chemie* **2006,** *45* (48), 8241-4.
10. Caixia Xu, J. S., Xiaohong Xu, Pengpeng Liu, Hongjuan Zhao, Fang Tian, and Yi Ding, Low Temperature CO Oxidation over Unsupported Nanoporous Gold. *Journal of the American Chemical Society* **2007,** *129*, 42-43.
11. Wittstock, A.; Wichmann, A.; Biener, J.; Bäumer, M., Nanoporous gold: a new gold catalyst with tunable properties. *Faraday Discussions* **2011,** *152*, 87.
12. Wittstock, A.; Zielasek, V.; Biener, J.; Friend, C. M.; Baumer, M., Nanoporous Gold Catalysts for Selective Gas-Phase Oxidative Coupling of Methanol at Low Temperature. *Science* **2010,** *327* (5963), 319-322.
13. Kosuda, K. M.; Wittstock, A.; Friend, C. M.; Bäumer, M., Oxygen-Mediated Coupling of Alcohols over Nanoporous Gold Catalysts at Ambient Pressures. *Angewandte Chemie International Edition* **2012,** *51* (7), 1698-1701.
14. Zugic, B.; Karakalos, S.; Stowers, K. J.; Biener, M. M.; Biener, J.; Madix, R. J.; Friend, C. M., Continuous Catalytic Production of Methyl Acrylates from Unsaturated Alcohols by Gold: The Strong Effect of C═C Unsaturation on Reaction Selectivity. *ACS Catalysis* **2016,** *6* (3), 1833-1839.
15. Personick, M. L.; Zugic, B.; Biener, M. M.; Biener, J.; Madix, R. J.; Friend, C. M., Ozone-Activated Nanoporous Gold: A Stable and Storable Material for Catalytic Oxidation. *ACS Catalysis* **2015,** *5* (7), 4237-4241.
16. Yan, M.; Jin, T.; Ishikawa, Y.; Minato, T.; Fujita, T.; Chen, L.-Y.; Bao, M.; Asao, N.; Chen, M.-W.; Yamamoto, Y., Nanoporous Gold Catalyst for Highly Selective Semihydrogenation of Alkynes: Remarkable Effect of Amine Additives. *Journal of the American Chemical Society* **2012,** *134* (42), 17536-17542.

17. Asao, N.; Ishikawa, Y.; Hatakeyama, N.; Menggenbateer; Yamamoto, Y.; Chen, M.; Zhang, W.; Inoue, A., Nanostructured Materials as Catalysts: Nanoporous-Gold-Catalyzed Oxidation of Organosilanes with Water. *Angewandte Chemie International Edition* **2010,** *49* (52), 10093-10095.

18. Jose A.Rodriguez, S. D. S.; Dario Stacchiola, P. L., and Jan Hrbek, The Activation of Gold and the Water Gas Shift Reaction: Insights from Studies with Model Catalysts. *Accounts of chemical research* **2013,** *47* (3), 773-782.

19. B. Hammer, J. K. N., Why gold is the noblest of all metals. *Nature* **1995,** *376*, 238-240.

20. Qiao, B.; Liang, J.-X.; Wang, A.; Xu, C.-Q.; Li, J.; Zhang, T.; Liu, J. J., Ultrastable single-atom gold catalysts with strong covalent metal-support interaction (CMSI). *Nano Research* **2015,** *8* (9), 2913-2924.

21. Hashmi, A. S. K., Sub-Nanosized Gold Catalysts. *Science* **2012,** *338* (6113), 1434-1434.

22. Matthey, D.; Wang, J. G.; Wendt, S.; Matthiesen, J.; Schaub, R.; Laegsgaard, E.; Hammer, B.; Besenbacher, F., Enhanced bonding of gold nanoparticles on oxidized TiO2(110). *Science* **2007,** *315* (5819), 1692-6.

23. Liu, P.; Rodriguez, J. A., Water-gas-shift reaction on metal nanoparticles and surfaces. *J Chem Phys* **2007,** *126* (16), 164705.

24. Fu, Q.; Saltsburg, H.; Flytzani-Stephanopoulos, M., Active nonmetallic Au and Pt species on ceria-based water-gas shift catalysts. *Science* **2003,** *301* (5635), 935-8.

25. Davis, R. J., Chemistry. All that glitters is not Au0. *Science* **2003,** *301* (5635), 926-7.

26. Rodriguez, J. A.; Wang, X.; Liu, P.; Wen, W.; Hanson, J. C.; Hrbek, J.; Pérez, M.; Evans, J., Gold nanoparticles on ceria: importance of O vacancies in the activation of gold. *Topics in Catalysis* **2007,** *44* (1-2), 73-81.

27. Norskov, J. K.; Bligaard, T.; Hvolbaek, B.; Abild-Pedersen, F.; Chorkendorff, I.; Christensen, C. H., The nature of the active site in heterogeneous metal catalysis. *Chemical Society reviews* **2008,** *37* (10), 2163-71.

28. Remediakis, I. N.; Lopez, N.; Nørskov, J. K., CO oxidation on gold nanoparticles: Theoretical studies. *Applied Catalysis A: General* **2005,** *291* (1-2), 13-20.

29. Arne Wittstock, B. N., Andreas Schaefer, Karifala Dumbuya, Christian Kuebel, Monika M. Biener, Volkmar Zielasek, Hans-Peter Steinruck, J. Michael Gottfried, Juergen Biener, Alex Hamza, and Marcus Baeumer, Nanoporous Au: An Unsupported Pure Gold Catalyst? *J. Phys. Chem. C* **2009,** *113*, 5593-5600.

30. Fujita, T.; Guan, P.; McKenna, K.; Lang, X.; Hirata, A.; Zhang, L.; Tokunaga, T.; Arai, S.; Yamamoto, Y.; Tanaka, N.; Ishikawa, Y.; Asao, N.; Yamamoto, Y.; Erlebacher, J.; Chen, M., Atomic origins of the high catalytic activity of nanoporous gold. *Nature Materials* **2012,** *11* (9), 775-780.

31. Asao, N.; Hatakeyama, N.; Menggenbateer; Minato, T.; Ito, E.; Hara, M.; Kim, Y.; Yamamoto, Y.; Chen, M.; Zhang, W.; Inoue, A., Aerobic oxidation of alcohols in the liquid phase with nanoporous gold catalysts. *Chemical communications* **2012,** *48* (38), 4540.

32. Fujita, T.; Tokunaga, T.; Zhang, L.; Li, D.; Chen, L.; Arai, S.; Yamamoto, Y.; Hirata, A.; Tanaka, N.; Ding, Y.; Chen, M., Atomic Observation of Catalysis-Induced Nanopore Coarsening of Nanoporous Gold. *Nano letters* **2014,** *14* (3), 1172-1177.

33. Haruta, M., New generation of gold catalysts: nanoporous foams and tubes -- is unsupported gold catalytically active? *Chemphyschem : a European journal of chemical physics and physical*

chemistry **2007,** *8* (13), 1911-3.

34. Moskaleva, L. V.; Röhe, S.; Wittstock, A.; Zielasek, V.; Klüner, T.; Neyman, K. M.; Bäumer, M., Silver residues as a possible key to a remarkable oxidative catalytic activity of nanoporous gold. *Physical Chemistry Chemical Physics* **2011,** *13* (10), 4529.

35. MADIX, A. G. S. a. R. J., Adsorption of oxygen and hydrogen on Au (110)-(1x2). *Surface Science* **1986,** *169*, 347-356.

36. Jooho Kim, E. S., and Bruce E. Koel, CO Adsorption and Reaction on Clean and Oxygen-Covered Au(211) Surfaces. *J. Phys. Chem. B* **2006,** *110*, 17512-17517.

37. Gawande, M. B.; Pandey, R. K.; Jayaram, R. V., Role of mixed metal oxides in catalysis science—versatile applications in organic synthesis. *Catalysis Science & Technology* **2012,** *2* (6), 1113.

38. Stacchiola, D. J.; Senanayake, S. D.; Liu, P.; Rodriguez, J. A., Fundamental studies of well-defined surfaces of mixed-metal oxides: special properties of MO(x)/TiO2(110) {M = V, Ru, Ce, or W}. *Chemical reviews* **2013,** *113* (6), 4373-90.

39. Shi, J., On the Synergetic Catalytic Effect in Heterogeneous Nanocomposite Catalysts. *Chemical reviews* **2013,** *113* (3), 2139-2181.

40. Shi, J.; Schaefer, A.; Wichmann, A.; Murshed, M. M.; Gesing, T. M.; Wittstock, A.; Bäumer, M., Nanoporous Gold-Supported Ceria for the Water–Gas Shift Reaction: UHV Inspired Design for Applied Catalysis. *The Journal of Physical Chemistry C* **2014,** *118* (50), 29270-29277.

41. Shi, J.; Mahr, C.; Murshed, M. M.; Zielasek, V.; Rosenauer, A.; Gesing, T. M.; Bäumer, M.; Wittstock, A., A versatile sol–gel coating for mixed oxides on nanoporous gold and their application in the water gas shift reaction. *Catal. Sci. Technol.* **2016**.

42. Ling Zhang, H. C., Akihiko Hirata, Hongkai Wu, Qi-Kun Xue, and Mingwei Chen, NanoporousGold BasedOptical Sensor for Sub-ppt Detection of Mercury Ions. *ACS nano* **2013,** *7* (5), 4595-4600.

43. Park, J. B.; Graciani, J.; Evans, J.; Stacchiola, D.; Ma, S.; Liu, P.; Nambu, A.; Sanz, J. F.; Hrbek, J.; Rodriguez, J. A., High catalytic activity of Au/CeOx/TiO2(110) controlled by the nature of the mixed-metal oxide at the nanometer level. *Proc. Natl. Acad. Sci. U. S. A.* **2009,** *106* (13), 4975-80.

44. J. A. Rodriguez, S. M., P. Liu, J. Hrbek, J. Evans, M. Pérez, Activity of CeOx and TiOx Nanoparticles Grown on Au(111) in the Water-Gas Shift Reaction. *Science* **2007,** *318*, 1757-1760.

45. Rodriguez, J. A.; Liu, P.; Hrbek, J.; Evans, J.; Perez, M., Water gas shift reaction on Cu and Au nanoparticles supported on CeO2(111) and ZnO(0001): intrinsic activity and importance of support interactions. *Angewandte Chemie* **2007,** *46* (8), 1329-32.

46. Rodríguez, J. A.; Hrbek, J., Inverse oxide/metal catalysts: A versatile approach for activity tests and mechanistic studies. *Surface Science* **2010,** *604* (3-4), 241-244.

47. Biener, M. M.; Biener, J.; Wichmann, A.; Wittstock, A.; Baumann, T. F.; Baumer, M.; Hamza, A. V., ALD functionalized nanoporous gold: thermal stability, mechanical properties, and catalytic activity. *Nano letters* **2011,** *11* (8), 3085-90.

48. Wichmann, A.; Wittstock, A.; Frank, K.; Biener, M. M.; Neumann, B.; Mädler, L.; Biener, J.; Rosenauer, A.; Bäumer, M., Maximizing Activity and Stability by Turning Gold Catalysis Upside Down: Oxide Particles on Nanoporous Gold. *ChemCatChem* **2013,** *5* (7), 2037-2043.

49. Lang, X.-Y.; Fu, H.-Y.; Hou, C.; Han, G.-F.; Yang, P.; Liu, Y.-B.; Jiang, Q., Nanoporous gold supported cobalt oxide microelectrodes as high-performance electrochemical biosensors. *Nature communications* **2013,** *4*.

50. Johnston-Peck, A. C.; Senanayake, S. D.; Plata, J. J.; Kundu, S.; Xu, W.; Barrio, L.; Graciani, J.; Sanz, J. F.; Navarro, R. M.; Fierro, J. L. G.; Stach, E. A.; Rodriguez, J. A., Nature of the Mixed-Oxide Interface in

Ceria–Titania Catalysts: Clusters, Chains, and Nanoparticles. *The Journal of Physical Chemistry C* **2013,** *117* (28), 14463-14471.

51. Li, S.; Zhu, H.; Qin, Z.; Wang, G.; Zhang, Y.; Wu, Z.; Li, Z.; Chen, G.; Dong, W.; Wu, Z.; Zheng, L.; Zhang, J.; Hu, T.; Wang, J., Morphologic effects of nano CeO2–TiO2 on the performance of Au/CeO2–TiO2 catalysts in low-temperature CO oxidation. *Applied Catalysis B: Environmental* **2014,** *144*, 498-506.

52. Shingo Watanabe, X. M., and Chunshan Song, Characterization of Structural and Surface Properties of Nanocrystalline TiO2 CeO2 Mixed Oxides by XRD, XPS, TPR, and TPD. *J. Phys. Chem. C* **2009,** *113*, 14249-14257.

53. Contreras-García, M. E.; García-Benjume, M. L.; Macías-Andrés, V. I.; Barajas-Ledesma, E.; Medina-Flores, A.; Espitia-Cabrera, M. I., Synergic effect of the TiO2-CeO2 nanoconjugate system on the band-gap for visible light photocatalysis. *Materials Science and Engineering: B* **2014,** *183*, 78-85.

54. Liu, Y.; Yao, W.; Cao, X.; Weng, X.; Wang, Y.; Wang, H.; Wu, Z., Supercritical water syntheses of CexTiO2 nano-catalysts with a strong metal-support interaction for selective catalytic reduction of NO with NH3. *Applied Catalysis B: Environmental* **2014,** *160-161*, 684-691.

55. Muñoz-Batista, M. J.; Gómez-Cerezo, M. N.; Kubacka, A.; Tudela, D.; Fernández-García, M., Role of Interface Contact in CeO2–TiO2Photocatalytic Composite Materials. *ACS Catalysis* **2014,** *4* (1), 63-72.

56. Shan, W.; Liu, F.; He, H.; Shi, X.; Zhang, C., An environmentally-benign CeO2-TiO2 catalyst for the selective catalytic reduction of NOx with NH3 in simulated diesel exhaust. *Catalysis Today* **2012,** *184* (1), 160-165.

57. Lamallem, M.; Ayadi, H. E.; Gennequin, C.; Cousin, R.; Siffert, S.; Aïssi, F.; Aboukaïs, A., Effect of the preparation method on Au/Ce-Ti-O catalysts activity for VOCs oxidation. *Catalysis Today* **2008,** *137* (2-4), 367-372.

58. Divya, S.; Nampoori, V. P. N.; Radhakrishnan, P.; Mujeeb, A., Intermediate Ce3+ defect level induced photoluminescence and third-order nonlinear optical effects in TiO2–CeO2 nanocomposites. *Applied Physics A* **2013,** *114* (2), 315-321.

59. Li, W.; Wang, F.; Feng, S.; Wang, J.; Sun, Z.; Li, B.; Li, Y.; Yang, J.; Elzatahry, A. A.; Xia, Y.; Zhao, D., Sol-gel design strategy for ultradispersed TiO2 nanoparticles on graphene for high-performance lithium ion batteries. *Journal of the American Chemical Society* **2013,** *135* (49), 18300-3.

60. Li, W.; Yang, J.; Wu, Z.; Wang, J.; Li, B.; Feng, S.; Deng, Y.; Zhang, F.; Zhao, D., A versatile kinetics-controlled coating method to construct uniform porous TiO2 shells for multifunctional core-shell structures. *Journal of the American Chemical Society* **2012,** *134* (29), 11864-7.

61. Schaefer, A.; Ragazzon, D.; Wittstock, A.; Walle, L. E.; Borg, A.; Bäumer, M.; Sandell, A., Toward Controlled Modification of Nanoporous Gold. A Detailed Surface Science Study on Cleaning and Oxidation. *The Journal of Physical Chemistry C* **2012,** *116* (7), 4564-4571.

62. Lee, Y.; He, G.; Akey, A. J.; Si, R.; Flytzani-Stephanopoulos, M.; Herman, I. P., Raman analysis of mode softening in nanoparticle CeO(2-delta) and Au-CeO(2-delta) during CO oxidation. *Journal of the American Chemical Society* **2011,** *133* (33), 12952-5.

63. Wu, Z.; Li, M.; Howe, J.; Meyer, H. M., 3rd; Overbury, S. H., Probing defect sites on CeO2 nanocrystals with well-defined surface planes by Raman spectroscopy and O2 adsorption. *Langmuir : the ACS journal of surfaces and colloids* **2010,** *26* (21), 16595-606.

64. Reddy, B. M.; Khan, A., Nanosized CeO2–SiO2, CeO2–TiO2, and CeO2–ZrO2 Mixed Oxides: Influence of Supporting Oxide on Thermal Stability and Oxygen Storage Properties of Ceria. *Catalysis*

Surveys from Asia **2005,** *9* (3), 155-171.

65. Saitzek, S.; Blach, J. F.; Villain, S.; Gavarri, J. R., Nanostructured ceria: a comparative study from X-ray diffraction, Raman spectroscopy and BET specific surface measurements. *physica status solidi (a)* **2008,** *205* (7), 1534-1539.

66. Filtschew, A.; Hofmann, K.; Hess, C., Ceria and Its Defect Structure: New Insights from a Combined Spectroscopic Approach. *The Journal of Physical Chemistry C* **2016,** *120* (12), 6694-6703.

67. McBride, J. R.; Hass, K. C.; Poindexter, B. D.; Weber, W. H., Raman and x-ray studies of Ce1−xRExO2−y, where RE=La, Pr, Nd, Eu, Gd, and Tb. *Journal of Applied Physics* **1994,** *76* (4), 2435.

68. Acerbi, N.; Golunski, S.; Tsang, S. C.; Daly, H.; Hardacre, C.; Smith, R.; Collier, P., Promotion of Ceria Catalysts by Precious Metals: Changes in Nature of the Interaction under Reducing and Oxidizing Conditions. *The Journal of Physical Chemistry C* **2012,** *116* (25), 13569-13583.

69. Chen, C. A.; Huang, Y. S.; Chung, W. H.; Tsai, D. S.; Tiong, K. K., Raman spectroscopy study of the phase transformation on nanocrystalline titania films prepared via metal organic vapour deposition. *Journal of Materials Science: Materials in Electronics* **2008,** *20* (S1), 303-306.

70. Hardcastle, F. D., Raman Spectroscopy of Titania (TiO2) NanotubularWater-Splitting Catalysts. *Journal of the Arkansas Academy of Science* **2011,** *65*, 43-48.

71. Frank, O.; Zukalova, M.; Laskova, B.; Kurti, J.; Koltai, J.; Kavan, L., Raman spectra of titanium dioxide (anatase, rutile) with identified oxygen isotopes (16, 17, 18). *Physical chemistry chemical physics : PCCP* **2012,** *14* (42), 14567-72.

72. Martos, M.; Julián‐López, B.; Folgado, J. V.; Cordoncillo, E.; Escribano, P., Sol‐Gel Synthesis of Tunable Cerium Titanate Materials. *European Journal of Inorganic Chemistry* **2008,** *2008* (20), 3163-3171.

73. Otsuka-Yao-Matsuo, S.; Omata, T.; Yoshimura, M., Photocatalytic behavior of cerium titanates, CeTiO4 and CeTi2O6 and their composite powders with SrTiO3. *Journal of Alloys and Compounds* **2004,** *376* (1-2), 262-267.

74. Benjaram M. Reddy, A. K., Yusuke Yamada, Tetsuhiko Kobayashi, Stephane Loridant and Jean-Claude Volta, Structural Characterization of CeO_2-TiO_2 and V_2O_5/CeO_2-TiO_2 Catalysts by Raman and XPS Techniques. *J. Phys. Chem. B* **2003,** *107*, 5162-5167.

75. Ratnasamy, C.; Wagner, J. P., Water Gas Shift Catalysis. *Catalysis Reviews* **2009,** *51* (3), 325-440.

76. Fu, Q.; Deng, W.; Saltsburg, H.; Flytzani-Stephanopoulos, M., Activity and stability of low-content gold–cerium oxide catalysts for the water–gas shift reaction. *Applied Catalysis B: Environmental* **2005,** *56* (1-2), 57-68.

77. Zhao, X.; Ma, S.; Hrbek, J.; Rodriguez, J. A., Reaction of water with Ce–Au(111) and CeOx/Au(111) surfaces: Photoemission and STM studies. *Surface Science* **2007,** *601* (12), 2445-2452.

78. Ma, S.; Rodriguez, J.; Hrbek, J., STM study of the growth of cerium oxide nanoparticles on Au(111). *Surface Science* **2008,** *602* (21), 3272-3278.

79. P. Dutta, S. P., and M. S. Seehra, Concentration of Ce 3+ and Oxygen Vacancies in Cerium Oxide Nanoparticles. *Chem. Mater.* **2006,** *18*, 5144-5146.

80. Si, R.; Tao, J.; Evans, J.; Park, J. B.; Barrio, L.; Hanson, J. C.; Zhu, Y.; Hrbek, J.; Rodriguez, J. A., Effect of Ceria on Gold–Titania Catalysts for the Water–Gas Shift Reaction: Fundamental Studies for Au/CeOx/TiO2(110) and Au/CeOx/TiO2Powders. *The Journal of Physical Chemistry C* **2012,** *116* (44), 23547-23555.

81. Yi, N.; Si, R.; Saltsburg, H.; Flytzani-Stephanopoulos, M., Active gold species on cerium oxide nanoshapes for methanol steam reforming and the water gas shift reactions. *Energy & Environmental Science* **2010,** *3* (6), 831.

82. Yi, N.; Si, R.; Saltsburg, H.; Flytzani-Stephanopoulos, M., Steam reforming of methanol over ceria and gold-ceria nanoshapes. *Applied Catalysis B: Environmental* **2010,** *95* (1-2), 87-92.

83. Yu, K. M.; Tong, W.; West, A.; Cheung, K.; Li, T.; Smith, G.; Guo, Y.; Tsang, S. C., Non-syngas direct steam reforming of methanol to hydrogen and carbon dioxide at low temperature. *Nature communications* **2012,** *3*, 1230.

84. Kusche, M.; Enzenberger, F.; Bajus, S.; Niedermeyer, H.; Bosmann, A.; Kaftan, A.; Laurin, M.; Libuda, J.; Wasserscheid, P., Enhanced activity and selectivity in catalytic methanol steam reforming by basic alkali metal salt coatings. *Angewandte Chemie* **2013,** *52* (19), 5028-32.

85. Matthew B. Boucher, N. Y., Forrest Gittleson, Branko Zugic, Howard Saltsburg, and Maria Flytzani-Stephanopoulos, Hydrogen Production from Methanol over Gold Supported on ZnO and CeO2 Nanoshapes. *J. Phys. Chem. C* **2011,** *115*, 1261-1268.

86. Papadopoulou, E.; Ioannides, T., Steam reforming of methanol over cobalt catalysts: Effect of cobalt oxidation state. *International Journal of Hydrogen Energy* **2015,** *40* (15), 5251-5255.

87. Barrios, C. E.; Bosco, M. V.; Baltanás, M. A.; Bonivardi, A. L., Hydrogen production by methanol steam reforming: Catalytic performance of supported-Pd on zinc–cerium oxides' nanocomposites. *Applied Catalysis B: Environmental* **2015,** *179*, 262-275.

88. Lin, S. D.; Cheng, H.; Hsiao, T. C., In situ DRIFTS study on the methanol oxidation by lattice oxygen over Cu/ZnO catalyst. *Journal of Molecular Catalysis A: Chemical* **2011,** *342-343*, 35-40.

89. Sá, S.; Silva, H.; Brandão, L.; Sousa, J. M.; Mendes, A., Catalysts for methanol steam reforming—A review. *Applied Catalysis B: Environmental* **2010,** *99* (1-2), 43-57.

90. Chiarello, G. L.; Aguirre, M. H.; Selli, E., Hydrogen production by photocatalytic steam reforming of methanol on noble metal-modified TiO2. *Journal of Catalysis* **2010,** *273* (2), 182-190.

91. Highfield, J. G.; Chen, M. H.; Nguyen, P. T.; Chen, Z., Mechanistic investigations of photo-driven processes over TiO2 by in-situ DRIFTS-MS: Part 1. Platinization and methanol reforming. *Energy & Environmental Science* **2009,** *2* (9), 991.

92. Wang, L.; Liu, Y.; Chen, M.; Cao, Y.; He, H.; Wu, G.; Dai, W.; Fan, K., Production of hydrogen by steam reforming of methanol over Cu/ZnO catalysts prepared via a practical soft reactive grinding route based on dry oxalate-precursor synthesis. *Journal of Catalysis* **2007,** *246* (1), 193-204.

93. Frank, B.; Jentoft, F.; Soerijanto, H.; Krohnert, J.; Schlogl, R.; Schomacker, R., Steam reforming of methanol over copper-containing catalysts: Influence of support material on microkinetics. *Journal of Catalysis* **2007,** *246* (1), 177-192.

94. Jacobs, G.; Patterson, P.; Graham, U.; Crawford, A.; Dozier, A.; Davis, B., Catalytic links among the water–gas shift, water-assisted formic acid decomposition, and methanol steam reforming reactions over Pt-promoted thoria. *Journal of Catalysis* **2005,** *235* (1), 79-91.

95. Jacobs, G.; Davis, B. H., In situ DRIFTS investigation of the steam reforming of methanol over Pt/ceria. *Applied Catalysis A: General* **2005,** *285* (1-2), 43-49.

96. Boccuzzi, F.; Chiorino, A.; Manzoli, M., FTIR study of methanol decomposition on gold catalyst for fuel cells. *Journal of Power Sources* **2003,** *118* (1-2), 304-310.

97. Haghofer, A.; Ferri, D.; Föttinger, K.; Rupprechter, G., Who Is Doing the Job? Unraveling the Role of Ga2O3in Methanol Steam Reforming on Pd2Ga/Ga2O3. *ACS Catalysis* **2012,** *2* (11), 2305-2315.

98. Tong, W.; Cheung, K.; West, A.; Yu, K. M.; Tsang, S. C., Direct methanol steam reforming to

hydrogen over CuZnGaOx catalysts without CO post-treatment: mechanistic considerations. *Physical chemistry chemical physics : PCCP* **2013,** *15* (19), 7240-8.

99. Huang, Y.; He, X.; Chen, Z.-X., Density functional study of methanol decomposition on clean and O or OH adsorbed PdZn(111). *The Journal of Chemical Physics* **2013,** *138* (18), 184701.

100. Lin, S.; Xie, D.; Guo, H., Pathways of Methanol Steam Reforming on PdZn and Comparison with Cu. *The Journal of Physical Chemistry C* **2011,** *115* (42), 20583-20589.

101. Manzoli, M.; Chiorino, A.; Boccuzzi, F., Decomposition and combined reforming of methanol to hydrogen: a FTIR and QMS study on Cu and Au catalysts supported on ZnO and TiO2. *Applied Catalysis B: Environmental* **2005,** *57* (3), 201-209.

102. Shi, J.; Mahr, C.; Murshed, M. M.; Gesing, T. M.; Rosenauer, A.; Baumer, M.; Wittstock, A., Steam reforming of methanol over oxide decorated nanoporous gold catalysts: a combined in situ FTIR and flow reactor study. *Physical chemistry chemical physics : PCCP* **2017**.

103. Brown, M. A.; Fujimori, Y.; Ringleb, F.; Shao, X.; Stavale, F.; Nilius, N.; Sterrer, M.; Freund, H. J., Oxidation of Au by surface OH: nucleation and electronic structure of gold on hydroxylated MgO(001). *Journal of the American Chemical Society* **2011,** *133* (27), 10668-76.

104. Davis, M. S. I. a. R. J., The Important Role of Hydroxyl on Oxidation Catalysis by Gold Nanoparticles. *Accounts of chemical research* **2014,** *47*, 825-833.

105. Wittstock, A.; Biener, J.; Bäumer, M., Nanoporous gold: a new material for catalytic and sensor applications. *Physical Chemistry Chemical Physics* **2010,** *12* (40), 12919.

106. Outka, D. A.; Madix, R. J., BRONSTED BASICITY OF ATOMIC OXYGEN ON THE AU(110) SURFACE - REACTIONS WITH METHANOL, ACETYLENE, WATER, AND ETHYLENE. *J. Am. Chem. Soc.* **1987,** *109* (6), 1708-1714.

107. Albrecht, P. M.; Mullins, D. R., Adsorption and Reaction of Methanol over CeOX(100) Thin Films. *Langmuir* **2013,** *29* (14), 4559-4567.

108. Lin, S.; Xie, D.; Guo, H., Methyl Formate Pathway in Methanol Steam Reforming on Copper: Density Functional Calculations. *ACS Catalysis* **2011,** *1* (10), 1263-1271.

109. Yang, X.; Kattel, S.; Senanayake, S. D.; Boscoboinik, J. A.; Nie, X.; Graciani, J.; Rodriguez, J. A.; Liu, P.; Stacchiola, D. J.; Chen, J. G., Low Pressure CO2 Hydrogenation to Methanol over Gold Nanoparticles Activated on a CeO(x)/TiO2 Interface. *Journal of the American Chemical Society* **2015,** *137* (32), 10104-7.

Junjie Shi

Personal data

- Born in ZiBo, ShanDong (China), October 15th, 1986.
- Address: Institute of Applied and Physical Chemistry, University Bremen, Leobener Str. NW2, 28359 Bremen, Germany.
- E-mail: junjieshiding@gmail.com or 407102565@qq.com

Education

- Since 2011 PhD Study at the Institute for Applied an Physical Chemistry at the University of Bremen, Germany
- 2009-2011 Master study at Desulphurization Laboratory at Ocean University of China, China
- 2005-2009 Bachelor study at Qingdao Agriculture University, China

Work experience

- 2013-2015 Lab training at the University of Bremen (Experimental course of physical chemistry)
- 2010-2011 Teaching assistantat Ocean University of China (Inorganic chemistry open experiment course)

Research Interests

Surface catalysis, Physical chemistry, catalytic studies under ambient conditions, innovative catalyst materials

Publications

1. **J. Shi**, A. Schaefer, A. Wichmann, M. M. Murshed, T. M. Gesing, A. Wittstock and M. Bäumer, Nanoporous Gold-Supported Ceria for the Water-Gas Shift Reaction: UHV Inspired Design for Applied Catalysis, The Journal of Physical Chemistry C, 118, 29270-29277, 2014.

2. **J. Shi**, Christoph Mahr, M. M. Murshed, T. M. Gesing, VolkmarZielasek, Andreas Rosenauer, A. Wittstock and M. Bäumer, A versatile sol-gel coating for mixed oxides on nanoporous gold and their application in the watergas shift reaction, Catalysis science & technology, 2016. DOI: 10.1039/C5CY02205C.

3. **Junjie Shi,** Christoph Mahr, M. Mangir Murshed, Thorsten M. Gesing, Andreas Rosenauer, Marcus Bäumer, Arne Wittstock, Steam Reforming of Methanol over Nanoporous Gold/Oxide Catalysts: A Combined In-situ FTIR and Flow Reactor Study, PCCP, 2017.

4. S. Baier, C. D. Damsgaard, M. Scholz, F. Benzi, A. Rochet, R. Hoppe, T. Scherer, **J. Shi,** A. Wittstock, B. Weinhausen , J. B. Wagner, C. G. Schroer and J.-D. Grunwaldt, "In situ ptychography of heterogeneous catalysts using hard X-rays: high resolution imaging at ambient pressure and elevated temperature", Microscopyand Microanalysis 22(1):178-188.

5. Sina Baier, Arne Wittstock, Christian D. Damsgaard, Ana Diaz, Juliane Reinhardt, Federico Benzi, **Junjie Shi**, Torsten Scherer, Di Wang, Christian Kübel, Christian G. Schroer and Jan-DierkGrunwaldt, Influence of gas atmosphere and ceria on the stability of nanoporous gold studied by environmental electron microscopy and in situ ptychograph, RSC advances, 2016, 6, 83031-83043.

6. Xue Yu, **Junjie Shi**, Wentai Wang, Liang Wang, JunjieBian, LijuanFeng, Chunhu Li, A novel Au NPs-loaded MoS_2/RGO composite for efficient hydrogen evolution under visible light, Materials letters, Volume 182, 1 November 2016, Pages 125–128.

7. Xue Yu, **Junjie Shi*(Corresponding)**, Lijuan Feng, Chunhu Li, Liang Wang*(Corresponding), “A Three-Dimensional BiOBr/RGO Heterostructural Aerogel with Enhanced and Selective Photocatalytic Properties under Visible Light”, Applied Surface Science, 2016.

Publication [I]

Nanoporous Gold-Supported Ceria for the Water–Gas Shift Reaction: UHV Inspired Design for Applied Catalysis

Junjie Shi, Andreas Schaefer, Andre Wichmann, M. Mangir Murshed, Thorsten M. Gesing, Arne Wittstock, and Marcus Bäumer

J. Phys. Chem. C, 2014, 118 (50), pp 29270–29277

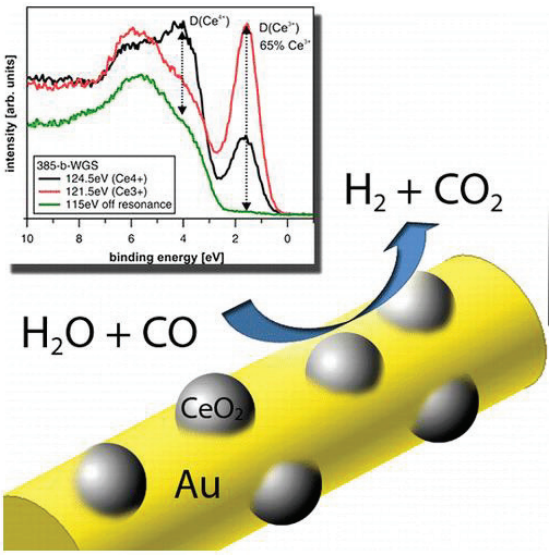

Publication [II]

A versatile sol–gel coating for mixed oxides on nanoporous gold and their application in the water gas shift reaction

Junjie Shi, Christoph Mahr, M. Mangir Murshed, Volkmar Zielasek, Andreas Rosenauer, Thorsten M. Gesing, Marcus Bäumer and Arne Wittstock

Catal. Sci. Technol., 2016, 6, 5311-5319

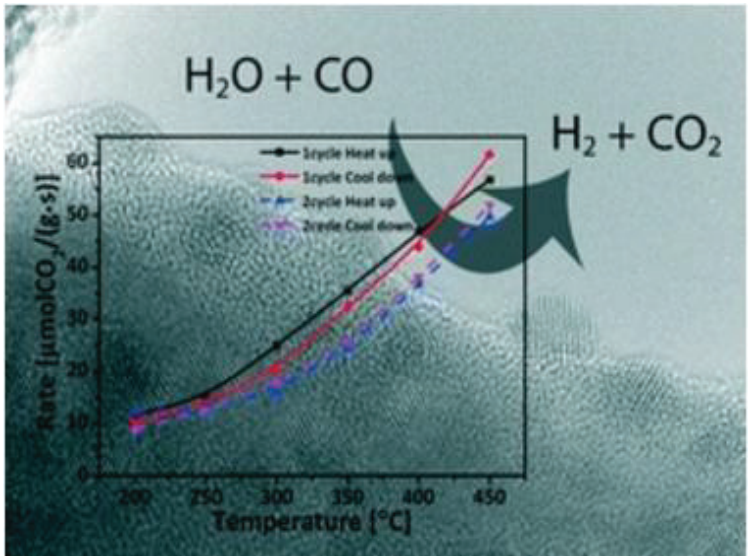

Published with open access. The publication can be accessed at: http://pubs.rsc.org/en/content/articlepdf/2016/cy/c5cy02205c

Publication [III]

Steam reforming of methanol over oxide decorated nanoporous gold catalysts: a combined in situ FTIR and flow reactor study

Junjie Shi, Christoph Mahr, M. Mangir Murshed, Thorsten M. Gesing, Andreas Rosenauer, Marcus Bäumer and Arne Wittstock

Phys. Chem. Chem. Phys., 2017,19, 8880-8888

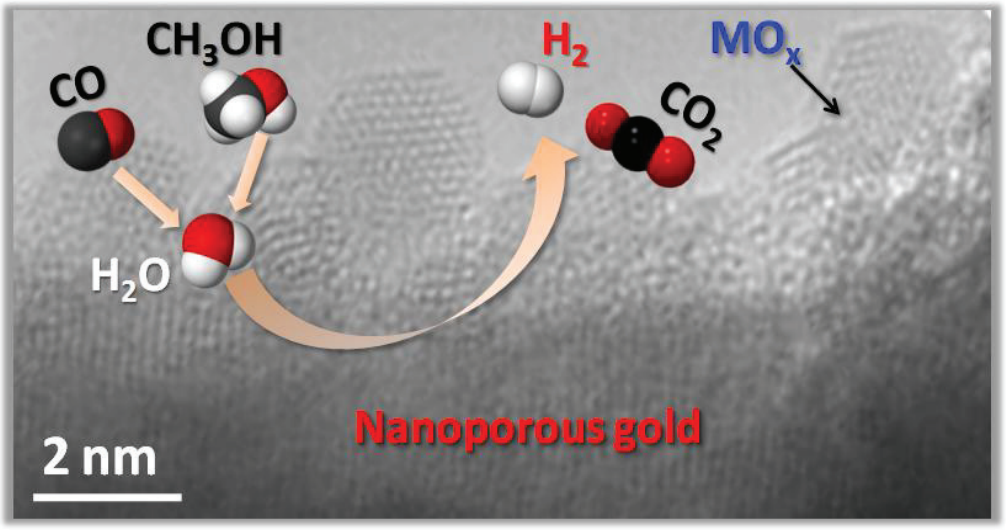

Publication [IV]

In Situ Ptychography of Heterogeneous Catalysts using Hard X-Rays: High Resolution Imaging at Ambient Pressure and Elevated Temperature

Sina Baier, Christian D. Damsgaard, Maria Scholz, Federico Benzi, Amélie Rochet, Robert Hoppe, Torsten Scherer, Junjie Shi, Arne Wittstock, Britta Weinhausen, Jakob B. Wagner, Christian G. Schroer and Jan-DierkGrunwaldt

Microscopy and Microanalysis, volume 22, issue 1 February 2016, pp. 178-188

Publication [V]

Influence of gas atmosphere and ceria on the stability of nanoporous gold studied by environmental electron microscopy and in situ ptychograph

Sina Baier, Arne Wittstock, Christian D. Damsgaard, Ana Diaz, Juliane Reinhardt, Federico Benzi, Junjie Shi, Torsten Scherer, Di Wang, Christian Kübel, Christian G. Schroerfi and Jan-Dierk Grunwaldt

RSC Adv., 2016, 6, 83031-83043